

**Potential Role for the Sarcolemmal Membrane Associated
Protein Isoform 3 (SLMAP3) in Cardiac Remodeling Post
Myocardial Infarction.**

By

Wafa Lefnaier

Department of Cellular and Molecular Medicine

Faculty of Medicine

University of Ottawa

Ottawa, Canada

January 09, 2017

A thesis submitted to the Faculty of Graduate and Postdoctoral Studies in partial fulfillment of the requirements for the M.Sc. degree in the Department of Cellular and Molecular Medicine.

© Wafa Lefnaier, Ottawa, Canada, 2017

ABSTRACT

The Sarcolemmal Membrane Associated Protein 3 (SLMAP3) is a tail-anchored membrane protein, which is ubiquitously expressed in tissues including myocardium. It is a component of subcellular membranes and the centrosome, and it appears to serve distinct roles in cell growth and membrane biology. In addition, mutations in SLMAP have been linked to Brugada syndrome, which leads to cardiac dysfunction and death. Here, we have examined the effects of different levels of SLMAP3 on postnatal heart function, pre and post myocardial infarction (MI). Transgenic (TG) mice with a cardiac specific expression of SLMAP3 isoform were generated and assessed with echocardiography to measure function, immunohistochemistry for histology, TUNEL assay for apoptosis, Masson's trichrome staining for fibrosis, and Western blots for protein expression.

Baseline echocardiography of 8 weeks old TG mice showed a normal cardiac function that was expressed in ejection fraction percent (%EF=66%±7.42), which was similar to those of wild type mice (%EF=67%±9.36), $p < 0.05$, $n = 20-25$ (in each group). MI was induced by permanent ligation of left anterior descending (LAD) artery in 9 week old WT & TG mice, while sham was the control. No death was recorded in SLMAP3 TG mice up to one year post MI, whereas 70% of WT mice had deceased, $p < 0.01$, $n = 17-18$ (in each group). Cardiac function was assessed by echocardiography (at 4 week post MI) showed a partially restored ejection fraction percent (%EF~49.2%±17.02) in SLMAP3 TG mice post MI compared to (%EF~36.4%±15.25) in WT mice post MI, $p < 0.05$, $n = 15-16$ (in each group). Furthermore, infarct size (IS) as well as collagen area (CA) post MI were significantly attenuated (IS~43%±8.82, CA~35%±5.15) in SLMAP3 TG myocardium in comparison to WT (IS~53%±9.30, CA~47%±7.36), $p < 0.05$, $n = 20-22$ (each group). Moreover, expression of the heart failure biomarker galectin3 was markedly

attenuated (1.8 ± 0.20) in SLMAP3 TG hearts post MI compared to (3.2 ± 0.35) in WT, $p < 0.01$, $n = 4-5$ (in each group). The apoptotic index in SLMAP3 TG myocardium assessed by TUNEL was markedly decreased (77 ± 11.48) in comparison to WT (112 ± 15.32), $p < 0.05$, ($n = 20-22$ in each group). Further, expression of proapoptotic proteins (Caspase3 and Bax) was significantly attenuated in SLMAP3 TG ($p < 0.05$, $n = 4-5$ in each group) while the expression of the prosurvival proteins (Bcl2 and caveolin3) was significantly upregulated ($p < 0.05$, $n = 4-5$ (in each group) in post MI. These data indicate that increased SLMAP3 levels serve to protect myocardium post MI through mechanisms which promote cell survival and limit cardiac fibrosis. Strategies to increase SLMAP3 level in myocardium may provide new therapeutic options in the treatment of heart failure.

ACKNOWLEDGMENTS

After an intensive period of 24 months today is the day: Writing this note of thanks is the finishing touch on my thesis. It has been a period of intense learning that has a big impact on me. I would like to reflect on the people who have supported me, not only in the scientific field, but also on a personal level.

I would first like to thank particularly my great mentor, Dr. Balwant Tuana, for his tremendous support and guidance in presenting this project. I would say to him "you supported me greatly and were willing to help me continuously".

I would like to thank specifically, my committee members, Dr. Patrick Burgon and Dr. Frans Leenen for their valuable advice and opinion throughout 2 years of time. Also, I would like to thank Rick Seymore in Heart Institute for his support in performing the animal's surgery in my project. Also, I would like to thank the staff in Pathology department at the University of Ottawa for their wonderful collaboration.

I would like to thank all of my colleagues in the lab, specifically Momena Dawood, Fernanda Gaisler, Jana Mlynarova, and Maysoon Salih, for their continuous advises. Also, I would like to thank my colleagues in the University of Ottawa especially in Dr. Lohnes lab for their wonderful support and advice.

Lastly, but not the least, I would also like to thank my amazing parents for their wise counsel and sympathetic ear. Special thanks to my lovely family, in particular my husband Nabil, my sons Ahmed and Aysam, and my daughter Alen. You are always there for me.

This work is dedicated to my family.

TABLE OF CONTENTS

ABSTRACT.....	ii
ACKNOWLEDEMENTS.....	iv
DEDICAION.....	v
TABLE OF CONTENTS.....	vi
LIST OF FIGURES.....	viii
LIST OF TABLES.....	ix
LIST OF ABBREVIATIONS.....	x

CHAPTER ONE

INTRODUCTION	1
1.1 Epidemiology of cardiovascular diseases.	1
1.2 Cardiac structure and circulations.	2
1.3 Cardiac nerve supply.	4
1.4 Cardiac metabolism and signal transduction inside cardiomyocyte.	5
1.4.1 Calcium regulation, Excitation-Contraction coupling and myocardial relaxation.	6
1.4.2 Physiological molecular mechanisms in the heart.	8
1.5 Molecular mechanisms post MI and pathogenesis of heart failure.	12
1.5.1 Necrosis and cellular injury post MI.	13
1.5.2 Inflammatory response and cellular infiltration in post MI.	14
1.5.3 Apoptotic pathways post MI.	15
1.5.4 Interstitial changes and fibrosis in post MI.	21
1.6 Sarcolemmal Membrane Associated Protein (SLMAP).	22
1.7 SLMAPs and various biological roles.	24
1.8 Disturbance of SLMAP expression and mutations in SLMAP gene implicated in clinical diseases.	28

1.9 Rationale and statement of problem.	30
<u>CHAPTER TWO</u>	
MATERIALS AND METHODS	32
2.1 Generation of SLMAP3 overexpressed transgenic mice and experimental animals	32
2.2 Genotyping	32
2.3 MI mouse model and echocardiography	33
2.4 Experimental groups	34
2.5 Terminal deoxynucleotidyl-transferase-mediated dUTP nick end labelling (TUNEL) assay	34
2.6 Masson's trichrome staining	35
2.7 Immunohistochemistry	36
2.8 Western blotting	36
2.9 Other parameters	37
2.10 Statistical analysis	38
<u>CHAPTER THREE</u>	
RESULTS	39
3.1 Generation of SLMAP3-TM2 transgenic mice	39
3.2 Baseline cardiac phenotype and histology	41
3.3 Cardiac function 4 weeks post MI was preserved by SLMAP3 overexpression	44
3.4 Kaplan Meier curve of SLMAP3 TG mice post MI	47
3.5 HF biomarker galectin3 was markedly reduced in SLMAP3 hearts	48
3.6 Collagen levels and infarct size were reduced by SLMAP3 in post MI	51
3.7 Apoptosis was attenuated in SLMAP3 myocardium post MI	55
3.8 SLMAP3 reduced prodeath and enhanced prosurvival signals post MI	57
3.9 Cav3 expression was enhanced, while ERK1/2 signaling mechanism of HF was depressed in SLMAP3 TG mice post MI	58
<u>CHAPTER FOUR</u>	
DISCUSSION	67
<u>CHAPTER FIVE</u>	
REFERENCES	75

LIST OF FIGURES

Figure 1: Extrinsic and intrinsic pathways of apoptosis	20
Figure 2: Generation of SLMAP3-TM2 TG mice	40
Figure 3: Cardiac phenotype of SLMAP3 TG mice	42
Figure 4: Echocardiography of 13 week old mice post MI	45
Figure 5: Kaplan Meier curve in SLMAP3 TG mice post MI	47
Figure 6: Heart failure biomarker “galectin3” expression in SLMAP3 TG hearts post MI	49
Figure 7: Cardiac fibrosis and infarct size in SLMAP3 TG myocardium post MI	52
Figure 8: Histology of mouse myocardium 1 year post MI	54
Figure 9: TUNEL assay of SLMAP3 TG myocardium post MI	56
Figure 10: Expression of endogenous SLMAP isoforms in the remote area post MI	59
Figure 11: Expression of SLMAP3 protein in different areas of left ventricle (I, B, R) post MI	60
Figure 12: Expression of proapoptotic and antiapoptotic proteins in infarct area (I) post MI	61
Figure 13: Expression of cardiac signaling proteins in infarct area post MI	62
Figure 14: Expression of proapoptotic and antiapoptotic proteins in border area (B) post MI	63
Figure 15: Expression of cardiac signaling proteins in border area post MI	64
Figure 16: Expression of proapoptotic and antiapoptotic proteins in remote area (R) post MI	65
Figure 17: Expression of cardiac signaling proteins in remote area post MI	66

LIST OF TABLES

Table 1: Functional analysis 4 weeks post MI

45

LIST OF ABBREVIATIONS

ANF: Atrial natriuretic factor
Apaf-1: Apoptotic protease activating factor 1
ATP: Adenosine triphosphate
AV: Atrioventricular
B: Border area
Bad: Bcl2-Associated death promoter protein
Bax: Bcl2 associated x protein
BCA: Bicinchoninic acid protein
Bcl2: Beta cell lymphoma 2 protein
B-MHC: Beta myosin heavy chain
BSA: Bovine serum albumin
BW: Body weight
cAMP: cyclic Adenosine monophosphate
CA: Collagen area
Ca⁺⁺: Calcium
CAL: Coronary artery ligation
Cav-3: Caveolin3
CK: Creatine kinase
CO₂: Carbon dioxide
CVDs: Cardiovascular diseases
DAB: 3, 3-diaminobenzidine
DM: Diabetes mellitus
DNA: Deoxyribonucleic acid
EF: Ejection fraction

E-C: Excitation-contraction
ECG: Electrocardiogram
ECM: Extracellular matrix
EDTA: Ethylene diamine tetra-acetic acid
EGF: Epidermal growth factor
EGTA: Ethylene glycol-bis(β -aminoethyl ether)-N,N,N',N'-tetraacetic acid
eNOS: endothelial nitric oxide synthase
ERK1/2: Extracellular signal-regulated kinases
FHA: forkhead-associated
FS: Fractional shortening
GAPDH: Glyceraldehyde 3-phosphate dehydrogenase
GDP: Guanosine diphosphate
GFP: Green fluorescent protein
GLUT4: Glucose transporter 4
G-Protein: GTP binding protein
GPCR: G-protein coupled receptor
GTP: Guanosine triphosphate
HF: Heart failure
H⁺: Hydrogen
H&E: Hematoxylin and eosin
HR: Heart rate
HRP: Horseradish peroxidase
HSP70: Heat shock protein 70
HW: Heart weight
IAPs: Inhibitor of apoptosis proteins

I: Infarct area
ILs: Interleukins
IS: Infarct size
IVS: Interventricular septum
JNK: c-Jun N-terminal kinase
K⁺: Kalium for potassium
KCL: Potassium chloride
LAD: Left anterior descending coronary artery
LDH: Lactic dehydrogenase
LW: Lung weight
LV: Left ventricle
LVEDD: Left ventricular end diastolic diameter
LVESD: Left ventricular end systolic diameter
LV WT;d: Left ventricular wall thickness in diastole
LV WT;s: Left ventricular wall thickness in systole
LZ: Leucine zipper
MAPK: Mitogen-activated protein kinase
MI: Myocardial infarction
µg: Microgram
µm: Micrometer
mM: Milli-molars
µL: Microliter
ml: milliliter
mm: Millimeter
MOM: Mitochondrial outer membrane

MPPs: Metalloproteinases
Na⁺: Sodium
NaCl: Sodium chloride
NaVO₄: Sodium valproate
NO: Nitric oxide
PBS: Phosphate-buffered saline
PCR: Polymerase chain reaction
P-ERK1/2: Phosphorylated ERK1/2
pH: Potential of hydrogen
PKA: Protein kinase A
PKC: Protein kinase C
PKG: Protein kinase G
PLN: Phospholamban
PTK: Protein tyrosine kinase
P value: Probability value
PVDF: Polyvinylidene difluoride
R: Remote area
RTK: Receptor tyrosine kinase
RyR2: Ryanodine receptor 2
SA: Sinoatrial
SAPK: Stress-activated protein kinase
SCNA5: Sodium voltage-gated channel alpha subunit 5
SDS-PAGE: Sodium dodecyl sulfate-Polyacrylamide gel electrophoresis
SED: Standard error of a difference
SERCA2a: Sarco/endoplasmic reticulum Calcium-ATPase 2a

siRNA: small interfering ribonucleic acid

SL: Sarcolemma

SLMAP: Sarcolemmal membrane associated protein

SNP: Single nucleotide polymorphism

SR: Sarcoplasmic reticulum

TBST: Tris-buffered saline tween

TdT: Terminal deoxynucleotidyl transferase

T-ERK1/2: Total ERK1/2

TM: Transmembrane

TG: Transgenic

TG MI: Transgenic myocardial infarction

TNF: Tumor necrosis factor

TNFR: Tumor necrosis factor receptor

Tris-HCL: Tris(hydroxymethyl) aminomethane-hydrochloric acid

TUNEL: Terminal deoxynucleotidyl-transferase-mediated dUTP nick end labelling

WHO: World health organization

WT: Wild type

WT MI: Wild type myocardial infarction

CHAPTER 1: INTRODUCTION

1.1 Epidemiology of cardiovascular diseases

Cardiovascular diseases (CVDs) are the leading cause of morbidity and mortality worldwide, and their prevalence continues to increase (Eapen et al., 2012). This group of diseases includes: myocardial infarction, cardiac failure, high blood pressure, stroke and peripheral vascular diseases (Eapen et al., 2012). Myocardial infarction (MI) and subsequent heart failure (HF) represent the highest proportion of CVDs and account for mortality rate of ~55% among these diseases (Eapen et al., 2012). MI accounts for ~12% of all deaths all over the world (WHO). There are many risk factors increasing the chance of development of heart disease such as: aging, genetic background of heart diseases, cigarette smoking, obesity, diabetes mellitus, high lipid profile and a sedentary life style (Rubin et al., 2005).

Myocardial infarct (MI) is the ischemic necrosis of cardiac tissue because of complete cessation of its blood supply mostly by thromboembolism (Ahmed et al., 2007). In MI, the infarcted tissue becomes poorly contracted and bulges outside during systole (Rubin et al., 2005). This results in a reduced pumping capacity of the heart, and rather than delivering blood to systemic circulation, blood accumulates in the heart and heart failure (HF) eventually develops (Rubin et al., 2005). Severity of HF and its manifestation depends on the percentage of ischemic myocardium, which affects the ventricle, and the duration of ischemia. When infarct involves ~50% of the left ventricle, cardiogenic shock is the most likelihood complication with mortality rate as high as 90% (Rubin et al., 2005). If the ischemic event extends beyond ~30 minutes, progressive and irreversible death of cardiomyocytes occurs, which leads to ventricular remodeling (Rubin et al., 2005). Despite the advanced interventional progress in management

options of MI and HF made over last few years, there is no cure for these diseases. Thus, all possible mechanisms that might be involved in pathogenesis of MI should be clearly understood in order to identify new target strategies in the future.

1.2 Cardiac structure and circulations

Heart is automated dynamic organ and has four chambers: right atrium, right ventricle, left atrium and left ventricle (McCance et al., 2010). The atria, or what are known auricles, have thin walls, while the ventricles have thicker walls, which mainly form the mass of the heart (McCance et al., 2010). The left ventricle is almost as much as three times the size of the right ventricle wall in thickness, and pumps the blood to all tissues (systemic circulation) through the aorta, while the right ventricle pumps the blood through pulmonary artery to lungs in a process known as pulmonary circulation (McCance et al., 2010).

In systemic circulation during systole, the left ventricle supplies all the tissues with oxygenated blood rich in nutrients, whereas during diastole the non-oxygenated blood, which is rich of CO₂, returns back from these tissues to the right atrium through superior and inferior vena cava (McCance et al., 2010).

Consecutively in pulmonary circulation during systole, the right ventricle pumps the non-oxygenated blood to the lungs through the pulmonary artery, where the blood gets oxygenated in the lungs, while in diastole the oxygenated blood returns back from lungs through pulmonary veins to the left atrium and then directly to the left ventricle through the mitral valve and in turn the systemic circulation begins again (McCance et al., 2010). Even though the heart is full of blood to supply all the systemic organs with oxygen and nutrients, interestingly the oxygen cannot be delivered directly to the cardiac cells through this direct way (McCance et al., 2010).

Instead, the heart gets nourished in an indirect way from the blood coming from the systemic circulation during diastole through coronary arteries, which originally branches from thoracic aorta into the right and left coronary sinuses (McCance et al., 2010).

In the coronary circulation during cardiac diastole, oxygenated blood flows from aorta to coronary sinuses and then to right and left coronary arteries connectively (Kumar & Clark, 2009). The right coronary artery arises from the right coronary sinus and supplies the right atrium and the right ventricle through its smaller branches, and continues to the posterior descending coronary artery to supply the posterior part of the interventricular septum and posterior wall of the left ventricle (Kumar & Clark, 2009). The left main coronary artery arises from left coronary sinus and divides into two branches; the left anterior descending artery (LAD), which supplies the anterior interventricular septum and the anterior wall of the left ventricle; and the circumflex artery which supplies the left atrium and the margins of the left ventricle through smaller branches (Kumar & Clark, 2009).

Another important circulation in the heart is the collateral circulation. This represents the anastomoses or the continuation between any of the coronary arteries (McCance et al., 2010). Collaterals vary from person to person in number and anatomical distribution, but they are mainly present in cardiac apex, anterior wall of right ventricle, interventricular & inter-atrial septa, and the epicardium (McCance et al., 2010). When one of the major coronary vessels occludes, the collaterals work instead to supply heart with the blood (Kumar & Clark, 2009). The more distributed the collaterals, the less chance to get an infarction. The clinical significance of these collaterals was introduced quite some time ago in 1960, when it was named the “collateral circulation protects the heart” (McCance et al., 2010). Clinical trials toward discovering mechanisms to enhance growing of new collaterals (angiogenesis) were introduced

to find new therapeutics to limit cardiac remodeling post MI. In vivo study, relaxin therapy post MI found to increase survival and reduce ventricular remodeling via enhancing the cardiac blood flow due to vasodilation of coronary arteries and stimulation of new blood vessel growth (Samuel et al., 2006). The underlying mechanism by which relaxin produced its effect is due to upregulation of vascular endothelial growth factor in response to nitric oxide (NO) signaling (Samuel et al., 2006). Although angiogenesis is not the only mechanism by which relaxin ameliorates the post MI remodeling, but it is still one of the major promising ones (Samuel et al., 2011, 2006).

Any factors that affect coronary circulation will impair the cardiac blood supply and might proceed to an ischemic event and MI (McCance et al., 2010). Some of these factors are blood pressure instability, either hypotension or hypertension due to stagnation of blood and degenerative changes respectively, and other metabolic factors such as high cholesterol blood level, which leads to atherosclerosis (Cotran & Robbins, 1997). Hypercholesteremia leads to fibrofatty plaque formation in coronary arteries (atherosclerotic plaque), which might bleed and thrombose to cause thromboembolism and result in development of angina pectoris and MI (Cotran & Robbins, 1997). Atherosclerotic plaque formation in coronary blood vessels represents the main cause of MI, in which the inner wall of the artery undergoes degenerative changes that ends up with plaque formation, and thus occlusion of the coronary artery (Kumar & Clark, 2009). There are also uncommon causes such as coronary vasospasm and migrating emboli from (mitral valve, aortic valve, and coronary arteries) inflammations that impact the coronary arteries and cause ischemia in the heart (Cotran & Robbins, 1997).

1.3 Cardiac nerve supply

Autonomic nervous system is the principal nerve supply of the heart throughout sympathetic (adrenergic), and parasympathetic (cholinergic) nerves (Kumar & Clark, 2009). The adrenergic nerves mainly supply the atria, ventricles, and the conduction system (Kumar & Clark, 2009). Conduction system is a special modified muscle fibers of heart that are capable to beat autonomously, which constitute mainly of sinoatrial (SA) node, atrioventricular (AV) node, and bundle of Hiss that bifurcates to the right bundle branch and the left bundle branch (Kumar & Clark, 2009). Adrenergic innervation of the heart is mediated by β_1 & β_2 receptors, where β_1 increases heart function and β_2 dilates the blood vessels. These receptors respond to both adrenaline and noradrenaline to cause positive inotropic and chronotropic effects, to enhance cardiac contractility and heart rate as well as blood flow (Kumar & Clark, 2009).

The cholinergic innervation of the heart via the vagus nerve is mediated by M2 muscarinic receptors, which mainly supply the conduction system to slow up the heart rate, or in other words, it has a negative chronotropic effect on heart (Kumar & Clark, 2009). Under normal conditions, muscarinic vagal effects on cardiac function overcome adrenergic effects, which results in a slow heart rate. However, in certain stressful conditions, whether physiological such as fear and fight, or pathological such as ischemic changes of heart, adrenergic stimulation predominates the vagal effect and results in a fast heart rate (tachycardia) and increased-cardiac contractility to increase the oxygen supply to the cardiac tissues (Kumar & Clark, 2009).

1.4 Cardiac metabolism and signal transduction inside cardiomyocyte

As like any other tissues, a normal cardiac muscle produces energy from oxidative phosphorylation of mainly fatty acids (~60-90%), and the remaining from glucose, lactate, and ketones (Stanley et al., 2005). In contrary, the metabolic process alters in cardiac diseases such

as in the end stage HF, in which cardiac cells consume less fatty acids, and more glucose is utilized (glycolysis) to produce the required energy (Stanley et al., 2005). The oxidative phosphorylation of metabolites takes place in mitochondria, which produce adenosine triphosphate (ATP) as a source of energy (McCance et al., 2010). Under normal condition, the amount of ATP produced by oxidative phosphorylation meets the required energy for functioning heart (McCance et al., 2010). If the blood supply of the heart is diminished for any reason, the metabolic state of cardiomyocyte changes from aerobic to an anaerobic state (McCance et al., 2010). In the anaerobic metabolism, the cells metabolize the glucose and other metabolites inefficiently, which results in accumulation of harmful waste products and development of cardiac diseases (Kumar & Clark, 2009; McCance et al., 2010).

The produced energy will be utilized mainly in muscle contraction & relaxation, initiation & potentiation of action potential, molecular transport across the membranes, and biosynthesis of proteins (McCance et al., 2010). When coronary blood supply to the heart is diminished, less oxygen will be delivered into cells, which will trigger the release of local metabolic factors such as adenosine (Kumar & Clark, 2009). These factors cause a coronary vasodilation as a compensatory mechanism from the heart in order to increase the blood flow, even though the oxygen content in the dilated vessel is still the same (McCance et al., 2010). Many factors affect the oxygen content of coronary blood; some might increase it while others decrease it. For instance, regular exercising and hyperemia increase the oxygen content in coronary vessels, while lowered blood pressure and temperature as well as cardiopulmonary diseases decrease it (McCance et al., 2010).

1.4.1 Calcium regulation, Excitation-Contraction Coupling and myocardial relaxation

Calcium dynamics within cardiomyocyte are a major regulator that controls the excitation-contraction (E-C) apparatus and relaxation mechanisms (Duarte-Costa et al., 2014). Contraction and relaxation processes are initiated by adrenergic stimulation, which then triggers the calcium release from its main intracellular stores such as SR (Kumar & Clark, 2009).

Upon stimulation of beta-1 adrenergic receptors, action potential is initiated and propagated in the plasma membrane of cardiomyocyte, and this leads to the opening of membrane ion channels such as sodium (Na^+) and calcium (Ca^{++}) channels (McCance et al., 2010). Ca^{++} ions flow from interstitial space to enter inside cardiomyocyte via two types of calcium channels; L-type (long-lasting type), which is the main calcium channel in the heart; and T-type (transient one), which is the less common type (McCance et al., 2010). The transient calcium ions entered from extracellular space activate ryanodine receptors (RyR2), which then evoke the release of intracellular stored-calcium from SR (Mattiuzzi et al., 2015). After that, calcium ion diffuses into the cell, where it binds to troponin to form calcium-troponin complex (McCance et al., 2010). This complex moves the tropomyosin molecule from myosin, which leaves myosin filaments exposed to actin binding and myosin-actin cross bridging begins (McCance et al., 2010). When myosin slides on actin, this leads to shortening of muscle microfilaments, and the net effect is muscle contraction (Kumar & Clark, 2009; McCance et al., 2010).

Beta-adrenergic receptors are activated by catecholamines, and this leads to stimulation of PKA, which phosphorylates certain intracellular proteins that regulate the relaxation process such as phospholamban (PLN), troponin I, and C protein (Kumar & Clark, 2009; Molenaar et al., 2007). Further, phosphorylated PLN will activate the calcium uptake in the SR by an ATPase pump or what is known as SERCA2a, thus the cytoplasmic calcium will be trapped in SR, which results in cardiomyocyte relaxation (Kumar & Clark, 2009). In addition, Phosphorylation of

troponin leads to conformational changes, which result in binding of troponin to myosin to form tropomyosin molecule. The latter molecule prevents sliding of actin on myosin filaments, and thus enhances muscle relaxation (Kumar & Clark, 2009; McCance et al., 2010).

Calcium ion flux within cardiomyocyte plays a pivotal role in the regulation of cardiac contractile function (Duarte-Costa et al., 2014). Disturbance in calcium handling inside cardiomyocyte is strongly associated with cardiovascular diseases, while on other hand, mechanisms that preserve the calcium recycling inside cardiomyocyte in MI animal experiments have been found to be cardioprotective (Duarte-Costa et al., 2014; Makarewich et al., 2014).

1.4.2 Physiological molecular mechanisms in the heart

Heart is a highly organized organ, which is regulated by interactive system that comprises the cellular signal transduction. In order for the cells of heart and blood vessels to function properly, they must transfer the extracellular stimuli to the inside throughout receptors located on their surface membranes such as G-protein coupled receptors (GPCRs), which are the most important receptors in these cells (Dzimiri, 2002).

GPCRs are nearly involved in each regulatory process inside cells via their interaction with heterotrimeric GTP binding proteins (G-Proteins) (Dzimiri, 2002). GPCRs activation could be involved in normal physiological signaling in response to angiotensin II, endothelin-1, and catecholamines, and the net effect will be regulating the arterial blood pressure, renal vascular response, cardiac hypertrophy, cardiac contractility, and heart rate (Dzimiri, 2002). In contrast, these receptors could be involved in certain pathological condition such as cardiac hypertrophy, atherosclerosis, and hypertension, in response to different stimuli (Dzimiri, 2002; McCance et al., 2010).

Interaction of GPCR with G-protein leads to conformational changes in this protein, which promote the transformation of GTP to GDP, and results in the activation of certain membrane ion channels, and enzymes such as adenylate cyclase and phospholipases (Cabrera-Vera et al., 2003). The activated channels and enzymes act as effector molecules, which regulate the generation of second messengers such as cAMP inside cardiomyocyte (Cabrera-Vera et al., 2003). Furthermore, second messengers regulate the phosphorylation process either by kinases that phosphorylate intracellular protein substrates or contrarily by phosphatases that dephosphorylate those substrates, and thus the balance between both arms of phosphorylation process will decide the fate of intracellular protein function (Cohen, 2002). Serious cardiovascular diseases may result from critical imbalance between kinases and phosphatases signal transduction (Krupnick & Benovic, 1998).

Phosphorylation of proteins inside cardiac cells is controlled by numerous enzymes including kinases and phosphatases, which are encoded by ~3% of the human genome (Manning et al., 2002). The process is highly reversible, and therefore the same protein substrate could be phosphorylated by kinases and dephosphorylated by phosphatases (Manning et al., 2002). Most of kinases provide phosphate group to the protein substrate from ATP, which results in modification of the protein substrate, and thus the protein substrate activity is altered. In addition, targeting of kinases or phosphatases to subcellular locations will further provide a strict control for phosphorylation process, which in turn alters the intracellular protein substrate activities (Ruehr et al., 2004).

Kinases are classified into two main groups based on the phosphorylated amino acid of protein substrate; serine/threonine kinases and tyrosine kinases. Generally, kinases perform wide range of intracellular tasks throughout regulating the signal transduction, which mainly regulate

normal physiological cardiovascular functions and to some extent mediate pathological signal transduction (Kumar & Clark, 2009; Yin et al., 2003). Serine/threonine kinases include protein kinase A (PKA), protein kinase G (PKG), and protein kinase C (PKC) (Rosse et al., 2010). PKA regulates the physiological response of heart and blood vessels to catecholamines via cyclic adenosine monophosphate (cAMP) dependent signaling (Hausdorff et al., 1990). PKG mediates the signaling that reduce vascular tone such as nitric oxide via cyclic guanosine monophosphate (cGMP) dependent way (Barman et al., 2003; Lincoln et al., 2001). PKC through different regulatory mechanisms could impact physiological and pathological signals in the heart depending on its downstream distribution (Rosse et al., 2010). PKC could protect the heart against the prolonged effect of ischemia via enhancing expression of some protective genes, and modulating the activity of apoptotic proteins (Penna et al., 2008). On the contrary, other studies have found that PKC in excessive amounts might prone cardiac cells to pathological hypertrophy and diseases, and when such a mechanism is prevented, a cardioprotection is achieved (Hahn et al., 2003; Markandeya et al., 2015). For instance, caveolin3 is one of the mechanisms that protect heart against pathological hypertrophy via number of signals; one of them was reducing calcium-mediated PKC signaling inside cardiomyocyte in the pathological cardiac hypertrophy mouse model (Markandeya et al., 2015).

Protein tyrosine kinases (PTKs) are large group of kinases, which phosphorylate tyrosine residue in proteins, and thus enhances the signal transduction inside the cells in response to ligand binding (Neet & Hunter, 1996). PTKs include receptor tyrosine kinases (RTKs) and non-receptor PTKs (Neet & Hunter, 1996; Yin et al., 2003). PTKs serve diverse roles such as cell growth, differentiation, metabolism, and cardiac protection against dilated cardiomyopathy (Crone et al., 2002; Yin et al., 2003).

Protein kinase cascades, regulate series of phosphorylation events inside the cardiomyocyte, thus providing a precise regulation of intracellular signaling pathways (English & Cobb, 2002). The kinase cascade responds to elevated cAMP levels with PKA stimulation, and acts as downstream signaling molecules to mediate further phosphorylation of intracellular proteins (Kumar & Clark, 2009). This group represents mitogen activated protein kinase (MAPK) cascades, which are one of the major serine/threonine kinases that regulate cascades of intracellular phosphorylation (English & Cobb, 2002; Kumar & Clark, 2009). MAPK cascades include MAPKs, MAPK kinases (MKKs), MAPK kinase kinase (MKKKs), which serve essential roles in signal transduction, augmentation, and inter-signaling crosstalk (Brondello et al., 1997).

The final molecule in kinase cascades is MAPK, which further phosphorylates plenty of intracellular proteins (Rosse et al., 2010). Subcellular targeting of MAPKs to various intracellular locations provides distinct cellular responses (Rosse et al., 2010). Scaffolding proteins inside the cells such as cav3 facilitate the physical interaction of MAPKs with each other, which determines the signaling selectivity and specificity (Burack & Shaw, 2000; Rosse et al., 2010). For instance, MAPKs could phosphorylate nuclear proteins and act as transcriptional factors, which provide a prolonged intracellular response by changing the gene expression (Su & Karin, 1996). On other hand, MAPKs could serve a rapid effect via phosphorylation of cytoplasmic proteins such as phospholipase A2 (Brand & Barton, 2002). MAPKs involve extracellular signal-regulated kinases (ERK1/2), p38 kinase, c-Jun N-terminal kinases/stress-activated protein kinases (JNK/SAPK), ERK3/4, and ERK5, which are mainly involved in cell growth, survival and apoptosis in response to different stimuli (Kumar & Clark, 2009; Zhang et al., 2016).

Interestingly, the molecular mechanisms in the heart have dual effects on the cardiovascular system, which could be involved in either physiological or pathological signaling pathways. Thus, downstream signal manipulation is very critical to alter the fate of the cellular responses either to accommodate to the physiological response or to fail and cardiac pathology develops.

1.5 Molecular mechanisms post MI and pathogenesis of heart failure

MI is a leading cause of death over the world, and patients who survive post MI are at great risk to develop heart failure (HF) throughout their lives (Kumar & Clark, 2009). HF is an eventual complication in post MI, in which the heart undergoes a series of pathological changes in a process known as cardiac remodeling (Eapen et al., 2012). The term cardiac remodeling, which refers to ventricular wall dilation, thinning, and stiffness, was first used by [(Pfeffer, Pfeffer, & Braunwald, 1985)]. In addition, ventricular remodeling also refers to cellular, molecular and interstitial changes that affect cardiomyocytes and other types of cardiac cells such as fibroblasts and vascular smooth myocytes in the infarcted area as well as the remote viable myocardium (Cohn et al., 2000; Kehat & Molkentin, 2010). Pathological cardiac hypertrophy either on cardiomyocyte level or on the heart level is also another characteristic of cardiac remodeling, in which the cardiomyocyte grows without a significant proliferation because the cardiomyocyte is already terminally differentiated (Kehat & Molkentin, 2010; Kumar & Clark, 2009). Cardiac remodeling is also associated with re-expression of some fetal genes, alteration in the metabolic state of cardiomyocytes, and alterations in the expression of proteins involved in excitation contraction coupling (Kehat & Molkentin, 2010; Kumar & Clark, 2009).

1.5.1 Necrosis and cellular injury post MI

Following occlusion of coronary artery, cardiac cells tolerate ischemic state for only 20 minutes, and then the cells start to die irreversibly without regulation in a process known as necrosis (McCance et al., 2010). During this time, cardiomyocytes metabolic state changed from an aerobic state to an anaerobic one, and this change could be reversible only if the blood supply returns to the infarct tissue within 20 minutes (McCance et al., 2010). In the anaerobic metabolism, cells utilize the stored glycogen as a source of energy in a process called glycolysis, which produce relatively less ATPs to meet the cardiac demands and contrarily more lactic acid is formed than in the aerobic metabolism (McCance et al., 2010). Accumulation of lactic acid inside cardiac cells lowers the pH, which in turn makes the cells more susceptible to degradation by proteolytic enzymes in lysosomes, and thus, more irreversible cellular death (necrosis) occurs (McCance et al., 2010). In necrotic death, cardiomyocytes undergo many changes such as loss of integrity of sarcolemma, which results in release of intracellular proteins such as troponins T&I isoforms, Lactic dehydrogenase (LDH) and creatinine Kinase (CK) (Cotran & Robbins, 1997). These proteins released to the plasma are biochemical markers used to detect MI (Cotran & Robbins, 1997).

Necrosis is a toxic and passive process, which is characterized by unprogrammed cell death and energy independence (McCance et al., 2010). Although this type of eventual cell death is hard to treat, revascularization or reperfusion therapy could help preventing necrosis partially, which is strictly time dependent and has no benefit of treatment when it has passed the early few hours of MI development (Reddy, 2015). In addition, reperfusion therapy has hazardous effects, and it is to some extent associated with an extensive cardiac injury in a condition named

reperfusion injury, in which the cardiac cells continue to commit suicide even though the blood supply is reinstated (Reddy, 2015).

As a result of necrosis, tissue cellular debris released to the adjacent myocardium, which attract immune and inflammatory cells at the periphery of infarct and the remote viable myocardium (Crocker & Murray, 2003). An extensive inflammatory process occurs in order to heal the wound at the margin of infarct, and it results in release of some chemicals, which trigger fibrosis and apoptosis (He et al., 2014; Mezzaroma et al., 2011). In apoptosis, the cardiac cells plan to die in a highly programmed way to save the intracellular structural ingredients until the blood supply returns to the infarct, otherwise if not, these cells eventually will be necrotized due to lack of energy (Crocker & Murray, 2003).

1.5.2 Inflammatory response and cellular infiltration in post MI

Within 24 hours after MI, white blood cells (leukocytes) begin to infiltrate to the margins of infarct, where they reach the maximum density on second to third day post MI (McCance et al., 2010). Leukocytes are mainly attracted to the border zone of infarct because there is still blood supply, and result in release of proteolytic enzymes that degrade the necrotic tissues, and attract more immune cells in a process known as karyorrhexis (Rubin et al., 2005). The immune cells start phagocytosis and engulf the periphery of the infarct and as a result, free radicals and cytokines released, which further mediate many immunological reactions at the periphery of infarct such as interstitial edema, microhemorrhage, apoptosis, and fibrosis (Kumar & Clark, 2009).

Inflammation is a well-known mechanism in post MI and leads to cardiac dysfunction and heart failure (Mezzaroma et al., 2011). Inflammation is initiated by ischemic injury in post

MI, and mediated by interleukins (ILs) and caspase-1, which further modulates the inflammatory response and promotes apoptosis in the border zone as well as the remote non-ischemic myocardium (Mezzaroma et al., 2011).

1.5.3 Apoptotic pathways post MI

Apoptosis is the programmed type of cell death in response to apoptotic stimuli such as ischemic injury, in which the cells protect their structures from their lysosomal enzymes, and thus reduce any further inflammatory reaction to prevent further breakdown of tissues (Crocker & Murray, 2003). In post MI, the apoptotic pathways are initiated when cardiac cells exposed to certain toxic substances originate from outside the cells in response to death receptor stimulation and called (external pathway), or from inside the cells in response to DNA damage and called (internal pathway).

In the external pathway, the apoptosis is triggered due to activation of membrane-bound death receptors, which include tumor necrosis factor receptors (TNFR) and Fas receptors in response to different stimuli such as cytokines released from inflammatory cells in post MI, which leads to caspase 8 activation (Gill et al., 2002). In turn, caspase 8 directly induce apoptosis, or indirectly by activating caspase 3, which itself mediates the apoptosis (Gill et al., 2002).

On other hand, intrinsic (mitochondrial) pathway of apoptosis is initiated by DNA damage, which triggers mitochondria to release cytochrome c to cytoplasm, and thus initiates apoptosis (Gill et al., 2002). Mitochondrial pathway is extremely controlled by intracellular regulators; some of them has inhibitory effect such as anti-apoptotic B cell lymphoma (Bcl2) protein, inhibitor of apoptosis (IAPs) proteins, growth factors; and some has stimulatory effect

such as proapoptotic proteins such as Bax, transcriptional factors, calcium overload and oxidants (Gill et al., 2002; Marín-García, 2016). In post MI, the balance between these regulators will determine the fate of cardiomyocytes whether to survive or to die (Marín-García, 2016).

For instance, when mitochondria is exposed to stress such as oxidants, this leads to changes in the mitochondrial outer membrane (MOM) permeability, which results in release of cytochrome c into cytoplasm (Crocker & Murray, 2003; Gill et al., 2002). Further, cytochrome c activates a cascade of proteins end up with an activation of caspase 3, which has a characteristic apoptotic activity (Shi, 2002). The mitochondrial pathway could be inhibited at several points by anti-apoptotic Bcl2 protein via stabilizing the MOM, and thus reducing its permeability, which in turn lowers cytochrome c release (Marín-García, 2016). On other hand, Bcl2 could work independently of cytochrome c release and reduce the cell death by binding to the apoptosis-activating factor (aPaf-1), and in turn reduce apoptosis (Desagher & Martinou, 2000; Rossé et al., 1998). In contrast, this pathway could be enhanced by proapoptotic proteins such as Bax, which is located to MOM (Marín-García, 2016). Bax alters mitochondrial transmembrane transition pores and increases the permeability of MOM, which results in cytochrome C release to cytoplasm (Marín-García, 2016). Further, cytochrome C interacts with Apaf-1 in presence of ATP, and results in apoptosome formation, which activates caspase 9 that activates the transforming of caspase 3 into cleaved caspase 3 (Amarante-Mendes et al., 1998; P. Li et al., 1997). Cleaved caspase 3 is a cysteine proteinase acts on aspartic acid residues, and breaks down many nuclear proteins such as DNA control proteins, cytoskeletal proteins, kinases, and inhibitors of endonucleases (Amarante-Mendes et al., 1998; P. Li et al., 1997). Finally, this results in degradation of nuclear membranes and fragmentation of the nuclei, and thus apoptosis occurs (Amarante-Mendes et al., 1998; Rossé et al., 1998).

Other factors inside the cell could affect the permeability of mitochondrial membranes, and thus change the fate of mitochondrial apoptosis. For instance, sudden calcium release from sarcoplasmic reticulum in response to oxidative stress and low pH inside the cells, leads to increased calcium release from mitochondria in calcium-induced calcium release mechanism, and thus increase the MOM permeability (Crompton, 1999). In contrary, there are some factors which might reduce the MOM permeability such as caveolin3, which acts as a scaffolding protein and enhances a cardioprotective mechanism (Hernandez-Resendiz & Zazueta, 2014). In the same study, cav3 contributed to cardioprotection in post ischemia/reperfusion injury in dilated cardiomyopathy animal model via increased trafficking of certain signaling complexes such as phospho-Akt, phospho-ERK1/2, and phospho-eNOS signaling pathways (Hernandez-Resendiz & Zazueta, 2014).

Although there is a cross talk between both pathways of apoptosis in activation of caspases family, Bcl2 family of proteins is still the major regulator of apoptosis that either serves as anti-apoptotic proteins such as: Bcl2, Bcl-XL, and Bcl-X, or as proapoptotic proteins such as: Bax and Bad, etc (Finucane et al., 1999). Thus, therefore the downstream regulation of these signaling molecules in apoptotic pathways will determine the degree of cell death and cardiac remodeling.

Extracellular signal-regulated kinases 1/2 (ERK1/2) pathway, which belongs to MAPKs kinases, is one of the major pathways involved in heart failure development (Kehat & Molkenin, 2010). The signal in cardiomyocyte is initiated at sarcolemma through the activation of GPCRs, receptor tyrosine kinases, and by stress stimuli (Bueno et al., 2000). Once ERK1/2 is activated, many intracellular proteins are phosphorylated such as transcription factors for fetal cardiac genes. However, ERK1/2 intracellular signaling in survival and apoptosis in certain cardiac

diseases is still under debate (Chuang et al., 2000; Kehat & Molkentin, 2010). Whereas ERK1/2 signals could enhance cellular growth, proliferation, and survival under stimulation of growth factors (Kehat & Molkentin, 2010), whilst on other hand, ERK1/2 pathways could be involved in apoptosis and pathological cardiac hypertrophy in response to stress stimuli such as in post MI stress (Iryo et al., 2000; Tuttolomondo et al., 2016). For instance, in the dilated cardiomyopathy mouse model study, extensive myocardial fibrosis and severe heart failure were notified in these mice, which were mediated by activation of ERK1/2 signaling that enhanced the expression of connective tissue growth factors (Chatzifrangkeskou et al., 2016). According to cell type and duration of ERK1/2 activation, along with the co-activated other intracellular pathways, ERK1/2 signalling responses differ (Mehrhof et al., 2001; Yeh et al., 2012).

In pathological cardiac hypertrophy, the ventricular cardiomyocyte undergoes subcellular remodeling concomitant with a reduction in caveolin3 (Cav-3) protein and altered calcium cycling (Alcalay et al., 2013; Tsutsumi et al., 2014). Caveolin3 is a key scaffolding protein for trafficking and stabilization of cardiac ion channels to plasma membrane as well as plays an important role in signal transduction within these cells (Cutler & Kaufman, 2013; Senatore et al., 2014). In Cutler's study, they have found that mutations in the Caveolin3 gene were associated with long QT syndrome, which lead to electrical cardiac dysfunction and death. Similar studies have linked these mutations to defects in nitric oxide synthase (NO synthase) and alteration in expression of sodium and potassium channels on cardiomyocytes, which lead to aberrant electrical activity and cardiac hypertrophic remodeling (Belge et al., 2014; Cutler & Kaufman, 2013; Senatore et al., 2014). In contrary, overexpression of Caveolin3 in HF animal model has improved the contractility of a failing heart via restoration of the distorted beta2-adrenergic receptor pool and its downstream calcium-cAMP signaling (Wright et al., 2014). Another study

on ischemia/reperfusion animal model has shown that Caveolin3 has a protective role in the heart against ischemia/reperfusion injury through activation of heat shock protein 70 (HSP 70) on mitochondrial levels (Tsutsumi et al., 2014).

However, apoptosis is strongly associated with ventricular dysfunction, remodeling and heart failure (Kumar & Clark, 2009). According to studies by Olivette and Wencker, the severity of heart failure was clinically relevant with the extent and degree of apoptosis in MI and HF experimental models (Olivetti et al., 1996; Wencker et al., 2003). Moreover, in the latter study, it was found that when myocyte's apoptosis was inhibited, the severity of heart failure lessened (Wencker et al., 2003). Further studies on experimental MI rodent model elucidated that inhibition of apoptosis was associated with less ventricular remodeling, and less inflammatory response concomitant with better cardiac function and survival (He et al., 2014; Ma et al., 2016). Therefore, finding mechanisms to suppress apoptosis in post MI and HF will provide a potential therapy for limiting ventricular remodeling and could improve the outcome of ischemic heart disease in the near future.

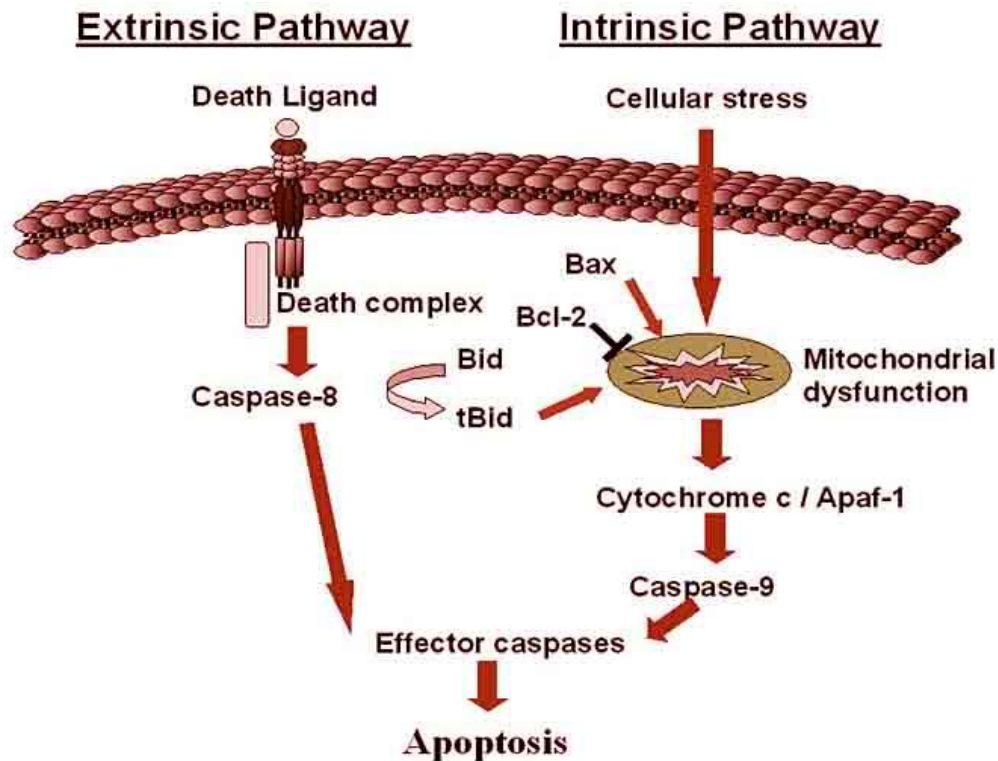


Figure 1: *Extrinsic and intrinsic pathways of apoptosis; in extrinsic pathway, the apoptosis is triggered due to activation of membrane-bound death receptors that form death complex, which leads to caspase 8 activation. Caspase 8 could directly induce apoptosis or indirectly by activating caspase 3, which mediates apoptosis. On other hand, the intrinsic pathway is initiated by cellular stress such as DNA damage, which leads to mitochondrial dysfunction, and thus cytochrome c release. Then, cytochrome c interacts with Apaf-1 to form the apoptosome, which activates cascade of caspases such as caspase 9 that activate the effector caspase 3, which mediate the apoptosis. The intrinsic apoptosis is further regulated by Bcl2 family of proteins, which includes the proapoptotic protein Bax and antiapoptotic protein Bcl2. Bax enhances release of cytochrome c through increasing the MOM permeability, while Bcl2 increases the stability of MOM, and thus reduces cytochrome c release. Figure is taken from Feldstein & Gores. (2005).*

1.5.4 Interstitial changes and fibrosis in post MI

When inflammatory signaling is suppressed and the number of inflammatory cells reduced, the profibrotic signaling will take over (Frangogiannis, 2008). Fibroblasts accumulate and proliferate on the fifth day post MI, which releases collagen gradually from the peripheral area of infarct toward its center, and this process takes around 4-6 weeks to become a well-established scar (Rubin et al., 2005). The newly deposited collagen within the first week of MI is delicate and liable to injury, and thus cardiac rupture may occur, which leads to sudden death (McCance et al., 2010). However, within 4-6 weeks post MI, the collagen becomes stronger and a well-established scar replaces the infarct necrotic tissue, which is resistant to injury, and thus cardiac rupture is less likelihood (Rubin et al., 2005).

In post MI, early fibroblasts in cardiac interstitial space produce matrix metalloproteinases (MMPs), which degrades the extracellular matrix (ECM), and thus allows an extensive attraction of inflammatory cells and macrophages (Frangogiannis, 2008; Kong et al., 2014). The macrophages engulf the degraded tissues and results in the release of TNF and interleukins (ILs) from these cells (Frangogiannis, 2008). ILs have a pleiotropic effect on numerous cell types in the heart mainly on fibroblasts (Frangogiannis, 2008; Kong et al., 2014). The newly formed fibroblasts then deposit new ECM proteins, mainly collagens at the margin of infarct toward its center (Kong et al., 2014; van den Borne et al., 2010). The early collagen deposited is type III, while the later one is type I (van den Borne et al., 2010). In vivo study of MI animal model has found that a notable fibrotic reaction extends beyond the infarct tissue to involve remote non-ischemic myocardium in response to inflammatory reaction, suggesting molecular-based signaling (Mezzaroma et al., 2011). In contrast, interventions that reduce excessive fibrosis post MI were found to reduce cardiac remodeling concomitantly with

increased survival rates as well as compensating the heart failure (Samuel et al., 2011). Hence, mechanisms that limit fibrosis post MI will provide a promising therapy.

1.6 Sarcolemmal Membrane Associated Protein (SLMAP)

SLMAP is a novel member of the superfamily of coiled-coil, tail-anchored membrane proteins, which are widely distributed in the tissues including myocardium (Wigle et al., 1997). SLMAPs could only be solubilized from cardiac membrane with detergents suggesting that they were integral membrane protein (Wigle et al., 1997). Further, immunohistochemical analysis of SLMAP protein in cardiac muscle has shown that SLMAP is localized in sarcolemma, transverse tubule, and sarcoplasmic reticulum, suggesting that this molecule can interact with important effector proteins to regulate various cell functions (Wigle et al., 1997). SLMAP has different isoforms (35,45, and 83-91 kDa) known as (SLMAP1, SLMAP2 and SLMAP3) encoded from three distinct mRNA transcript (3.5 kb, 4.5 kb, and 5.9 kb) from a single gene, which is located on the short arm of human chromosome 3 (3p14.3-21.2) (Wielowieyski et al., 2000; Wigle et al., 1997). This region of chromosome has found to be involved in regulation of cellular growth and development, and any abnormality in that area of chromosome 3 has been reported to be related to cancer (Ali et al., 1989). SLMAP gene comprises 24 exons spread over ~122 kb of DNA (Guzzo et al., 2004). SLMAP1 and SLMAP2 transcripts were mainly expressed in the heart, slow twitch soleus muscle and smooth muscles, while SLMAP3 transcript was ubiquitously expressed in tissues such as in the heart, brain, kidney, liver, muscles and pancreas as it was reported by Northern blot analysis (Wigle et al., 1997). Various transcripts of SLMAP are generated by alternative splicing mechanisms (Wielowieyski et al., 2000). SLMAP1 was encoded by 11 exons distributed over ~35 kilobase pairs of continuous DNA; 9 of the exons were constitutively expressed, and 2 were alternatively spliced (Wielowieyski et al., 2000). The

exons range from 60-321 base pairs, while the introns range from 0.2 to 10 kilobase pairs (Wielowieyski et al., 2000).

Structurally, SLMAP protein consists of a central alpha-helical coiled-coil domain, which is formed by two leucine zippers, and a hydrophobic carboxyl-terminal transmembrane (TM) domain (Wigle et al., 1997). The study of protein to protein interaction indicates that SLMAP proteins can self-assemble (homodimerize) and bind to other proteins in the membrane structures, and these interactions are mediated by the leucine-rich coiled-coil motifs (Guzzo et al., 2004). The characteristic feature of SLMAP proteins was their ability to form an extended coiled coil structure over most of their length (Wielowieyski et al., 2000; Wigle et al., 1997). The hydrophobic C-terminal in SLMAP molecule is alternatively spliced into TM1 or TM2, which further determines SLMAP subcellular targeting (Byers et al., 2009). For example; when TM1 is expressed, it introduces an in-frame stop codon, which makes the TM2 inactive (Byers et al., 2009).

The common localization of SLMAP encoding TM1 is sarcolemma, transverse tubules and sarcoplasmic reticulum (SR), while TM2 predominantly directs SLMAP to the mitochondrial outer membrane (MOM) as well as SR and this suggests that SLMAPs may serve different biological roles (Byers et al., 2009). Sequence analysis of SLMAP1 TM domain showed that only TM2 possessed positively charged residues (Byers et al., 2009). This suggested that the charge of amino acid residues, as well as the overall hydrophobicity profile of TM domain determines subcellular membrane targeting (Byers et al., 2009).

In addition to the previous common structure of SLMAPs, a 91 kDa SLMAP3 has a specific N-terminal sequence known as forkhead-associated (FHA) domain that localizes at the

centrosomes (Guzzo, Wigle, et al., 2004). Generally, forkhead-associated domain was found to play a vital role in regulation of cell growth, proliferation and immune response (Pike et al., 2001; Weng et al., 2015).

1.7 SLMAPs and various biological roles

Expression of SLMAP isoforms in tissue-specific manner has served wide range of vital roles in these tissues. 35 kDa SLMAP1 and 45 kDa SLMAP2 are mainly expressed in the heart, the slow twitch skeletal muscle (soleus), and smooth muscles, where it is believed to serve a unique role in these muscles (Wigle et al., 1997). In cardiomyocyte, SLMAPs were found to localize subcellular membranes such as sarcolemma, t-tubules and SR through carboxyl COOH-terminal membrane anchors (Guzzo et al., 2005). Furthermore, the cardiac-specific expression of SLMAPs revealed that these molecules that targeted distinct subcellular membranes were capable of self-assembling and interacting with the myofibrils, suggesting a potential role for this molecule in the structural arrangement of the excitation contraction (E-C) coupling apparatus (Guzzo et al., 2005). Furthermore, SLMAPs carrying either transmembrane domains found to be colocalized with caveolin3 and L-type calcium channels in sarcolemma as well as calcium-excreting channel ryanodine receptor (RyR2) of the sarcoplasmic reticulum (Guzzo et al., 2005).

Later in another study, the role of SLMAP in cardiac function and E-C coupling system was assessed, and it was found that SLMAP is a vital regulator of E-C coupling at the level of the SR and SL proteins, and disturbing the normal level of these proteins results in deterioration of cardiac electrophysiology and function (Nader et al., 2012). In this study, transgenic mice were created with cardiac specific overexpression of SLMAP1 encoding TM2 to interfere with the endogenous SLMAPs through homodimerization and subcellular targeting (Nader et al.,

2012). The young transgenic (TG) mice, at 5 weeks of age, showed mild cardiac dysfunction such as prolonged QT interval as recorded by electrocardiogram (ECG) as well as activation of cardiac remodeling genes like atrial natriuretic peptide (ANF) and β -MHC; while the older TG mice, which were about 28 weeks old, showed somewhat more cardiac dysfunction such as prolonged QT interval, reduced contractility with an impaired relaxation as assessed by left ventricle pressure monitoring (Nader et al., 2012). These TG mice also showed less response to isoproterenol challenge and developed left ventricular pressure alternans when compared to wild type mice (Nader et al., 2012). The cardiac function impairment seen in these TG mice was associated with low expression of calcium handling proteins in SR such as ryanodine receptor, calcium ATPase, calcineurin, and triadin, concomitant with significant reduction of calcium uptake in microsomal fractions (Nader et al., 2012). Furthermore, histological examination of these TG hearts revealed myocardium full of vacuoles, in which the severely vacuolated were associated with the higher expression level of SLMAP1-TM2 (Nader et al., 2012). Moreover, using high resolution microscope and biochemical analysis has found that SR was notably enlarged and SLMAP1-TM2 was targeted to SR membranes consecutively (Nader et al., 2012). These findings highlighted the vital role of SLMAP in the membrane biology of cardiac function, and found that regulated levels of this protein are critical for E-C coupling (Nader et al., 2012).

91 kDa SLMAP3 that has the specific N-terminal forkhead associated domain was found to be expressed ubiquitously in tissues including myocardium (Wigle et al., 1997). In vivo expression analysis found that SLMAP3-TM1 is present in somites (11 days post-coitum) as well as in fusing myotubes and localizes the SR and transverse tubules in adult skeletal muscles (Guzzo et al., 2004). Cryosections obtained from tissues of developing mice (11-18 days post-

coitum), and from adult skeletal muscles have shown that SLMAP is expressed in early development at 11 days post-coitum (Guzzo et al., 2004). In its early development (11 d.p.c), SLMAP was observed along the length of the myotube (Guzzo et al., 2004). Later in its development at (15 d.p.c) and before transition of myotube to myofibre, SLMAP expression was increased and organized in reticular pattern and fine longitudinal structures (Guzzo et al., 2004). Then at a later stage of development at (18 d.p.c), SLMAP was recognized in specific staining pattern, and was notably observed in skeletal muscles such as in adult tibialis anterior muscle (Guzzo et al., 2004). Moreover in early development, using double-immunofluorescent labelling, SLMAP was localized in subcellular structures of developing muscle and skeletal muscle where it was colocalized in some parts with an endoplasmic reticulum marker, but it was not colocalized with the Golgi body marker Golgin (Guzzo et al., 2004). In later development (at 18 d.p.c), SLMAP was also colocalized with myofibril Z-line marker in a striated pattern (Guzzo et al., 2004). Beyond (18 d.p.c) in the development, and in the mature skeletal muscle, SLMAP was seen in a continuous reticular distribution around and between the myofibrils, and as delicate longitudinal structures perpendicular to Z-lines (Guzzo et al., 2004). Furthermore in adult skeletal muscle, SLMAP was colocalized with Ca^{++} ATPase, the marker of SR longitudinal membranes, and partially with α -1 subunit of the DHP receptor, the marker of T-tubule as well as caveolin-3 the marker of the surface membrane (Guzzo et al., 2004). In Guzzo's study, skeletal muscle myoblasts were found to express a single 5.9 kb transcript, which encodes the full length ~91kDa SLMAP3 isoform. The myoblast differentiation was accompanied by stable expression of both ~91kDa SLMAP protein and ~80 kDa isoform (Guzzo et al., 2004). As SLMAPs deregulated by ectopic expression, the myoblast fusion was inhibited without any notable change in the muscle specific genes (Guzzo et al., 2004). Due to ability of SLMAPs to

self-assemble, the myotube formation was not inhibited unless the deregulated expression of mutants was not capable to homodimers (Guzzo et al., 2004). These findings concluded that regulated levels of SLMAP isoforms along with their temporal induction are important for normal muscle development (Guzzo et al., 2004).

The entire genomic structure of SLMAP gene was found to have 24 exons spread over ~122 kb of DNA, which encodes SLMAP3 isoform (Guzzo et al., 2004). In addition to the common structure of SLMAP isoforms that consists of a central coiled-coil alpha helical domain, 2 leucine zipper motifs, and alternatively spliced transmembrane domains, a 91 kDa SLMAP isoform (SLMAP3) has a specific N-terminus known as forkhead-associated domain (Guzzo et al., 2004). Generally, proteins that contain forkhead associated domain (FHA) are a family of transcriptional factors regulating gene expression involved in diverse biological role such as cell growth, proliferation, differentiation, immunity, and longevity (S. Li et al., 2016; Malo et al., 2016; Weng et al., 2015). FHA proteins play major roles in cardiogenesis and heart development of human embryo, and certain mutations in these genes could implicate development of congenital heart diseases (Zhu, 2016). SLMAP 3 isoform that encompass unique FHA domain found to be a component of microtubule organizing center (Guzzo et al., 2004). Co-immunostaining of cardiomyocytes in vitro study found that SLMAP3 N-terminus was co-localized with γ -tubulin the marker of centrosomes in all phases of cell cycle (Guzzo et al., 2004). Furthermore, when these cells were treated with agents that are well known to disrupt the centrosomes, association of SLMAP with the centrosomes wasn't affected (Guzzo et al., 2004). Moreover, a reporter green fluorescent protein (GFP) was targeted to SLMAP sequence to cause deletion mutation of newly identified N-terminal sequence from SLMAP, and this was found to stop the centrosomal targeting (Guzzo et al., 2004). This study concluded that high levels of

centrosomal SLMAP found to be lethal to cardiomyocytes, while mutants that were deficit in centrosomal targeting N-terminus found to suppress the cell growth, in which the cells were unable to divide and the cell cycle was arrested at G2/M phase (Guzzo et al., 2004).

1.8 Disturbance of SLMAP expression and mutations in SLMAP gene implicated in clinical diseases

Disturbed levels of the SLMAP protein as well as mutations in the SLMAP gene were found to be implicated in development of certain diseases such as type 2 diabetes mellitus (DM) and Brugada syndrome (Chen & Ding, 2011; Ishikawa et al., 2012). DM is a clinical disease characterized by high blood glucose level (hyperglycemia) due to absolute or relative deficiency of insulin (Kumar & Clark, 2009). DM is classified into two types; the first is type 1 diabetes mellitus, in which pancreas is no longer excreting insulin in the blood and thus results in hyperglycemia, and where insulin replacement therapy is necessary for patients to survive; secondly, there is type 2 diabetes mellitus, in which a hyperglycemic state results from reduction of insulin excretion from the pancreas and or the inability of body tissues to react to insulin or in other terms due to insulin resistance (Kumar & Clark, 2009). The insulin resistance in type 2 diabetes results from the desensitization of insulin receptors on the cell surface of body tissues such as adipose and muscular tissues (Kumar & Clark, 2009).

SLMAP plays major role in membrane biology and deregulated expression of SLMAP found to be associated in type 2 diabetes mellitus and its complication (Chen & Ding, 2011). Previous study on SLMAP (Ding et al., 2005) found that the microvasculature changes accompanied type 2 diabetes in the diabetic mouse model are correlated with high expression of aberrant SLMAPs. By contrast, when these changes were reversed, SLMAP significantly

reduced (Ding et al., 2005). These findings highlighted the contribution of disturbed SLMAP expression with the development of microvascular disease in type 2 diabetes (Ding et al., 2005). Further study in vivo has shown that 45 kDa and 35 KDa isoforms of SLMAP were upregulated in adipocyte extracted from adipose tissue of diabetic mice (Chen & Ding, 2011). This upregulation was significantly higher in mice with hyperglycaemic state than normoglycemic ones (Chen & Ding, 2011). Moreover, This change in SLMAP expression was associated with reduction in the expression of membrane glucose transporter (GLUT4), which plays a major role in transporting glucose from extracellular space to inside the cells (Chen & Ding, 2011). Furthermore, knocking down of SLMAP in adipocytes by small interfering RNA (siRNA) has been found to reduce the glucose uptake concomitantly with reduced SLMAP levels (Chen & Ding, 2011). These findings concluded that SLMAP is important molecule to regulate the glucose uptake via enhancing GLUT4 transportation across the membrane, and any disturbance in SLMAP levels might lead to diabetes (Chen & Ding, 2011). Other study on population suffering from diabetes has revealed that single nucleotide polymorphism (SNP) in SLMAP gene increases the risk to develop type 2 diabetes and diabetic retinopathy, which is one of the major complications of diabetes mellitus (Upadhyay et al., 2015).

Brugada syndrome is an inherited disease manifested clinically with an aberrant electrical activity leading to cardiac dysfunction and sudden death (Wilde et al., 2002). This disease was first notified in group of young patients that had a ventricular arrhythmia for no obvious clinical cardiac disease (Lemery et al., 1989). Those patients were followed up for recurrence and outcome of the disease (Lemery et al., 1989). Only one patient died because of cancer, while the remaining died because of recurrent cardiac arrhythmia and sudden death within the 8 years of study period (Lemery et al., 1989). The disease found to run in families in

an autosomal dominant mode of transmission, and characterized by the cardiac ion channels dysfunction including sodium (Na^+), calcium (Ca^{++}), potassium (K^+), and hydrogen (H^+) channels (Wilde et al., 2002). Defects in these channels lead to delayed action potential and early repolarization of cardiomyocyte plasma membrane (Wilde et al., 2002). This leads to a prolonged cardiac relaxation and cardiac arrest, which manifested clinically as prolonged QT, ST wave elevation, J wave appearance, and ventricular arrhythmia on ECG records (Wilde et al., 2002). Although many mutant genes encoding (Na^+ , Ca^{++} , K^+) channels are associated with Brugada syndrome, the mutations in the gene encoding sodium channel (SCNA5) are the most leading mutants found to be linked with Brugada syndrome (Antzelevitch & Patocskai, 2016; Wilde et al., 2002). Recently, two missense mutations (Val269Ile and Glu710Ala) in SLMAP gene have been linked to development of Brugada syndrome, which were not found in normal population (Ishikawa et al., 2012). These mutations in SLMAP have led to a decrease in expression of sodium channel (hNav1.5) on cardiomyocyte surface, and thus reduced the inward sodium current and initiation of action potential (Ishikawa et al., 2012). This study has found that there is no direct physical interaction of SLMAP with hNav1.5, suggesting that SLMAP functions indirectly via modulating the trafficking of hNav1.5 to cell surface (Ishikawa et al., 2012).

1.9 Rationale and statement of problem

MI and HF are leading causes of death worldwide, and up until recently, there is no valuable cure for these diseases. However, molecular mechanisms are highly involved in the development of cardiac remodeling in post MI, and certain manipulations target these mechanisms may provide a promising option for the treatment of MI in the future.

SLMAP is a component of cellular membranes and the microtubule organizing center, and it serves roles in cell growth, myoblast fusion, and excitation-contraction coupling through alteration of calcium handling proteins expression in cardiomyocytes. Moreover, disturbance in SLMAP expression and mutations in the protein have been implicated in certain diseases such as diabetes mellitus and Brugada syndrome.

Taking into consideration all the potential roles of SLMAP in cardiac membrane biology, regulation of E-C coupling, and cell growth, along with the fact that SLMAP mutations have implicated in development of serious cardiac disease (Brugada syndrome), it seems reasonable to postulate that SLMAP3 could be a determinant of normal cardiac function.

Hypothesis: Increased levels of SLMAP3 in the heart will either protect or be detrimental in post myocardial infarction, or were these mice better equipped to survive stress such as that imposed by MI.

In order to assess this hypothesis, my objectives were as follows:

- Induce MI in SLMAP3 transgenic (TG) mice and compare it with corresponding littermates of wild type (WT).
- Examine cardiac function in SLMAP3 transgenic mice post MI by echocardiography in comparison to WT littermates.
- Assess cardiac remodeling (fibrosis, apoptosis, and signaling) in SLMAP transgenic myocardium.
- Determine survival-death rates in SLMAP3 transgenic mice versus WT post MI.

CHAPTER 2: MATERIALS AND METHODS

2.1 Generation of SLMAP3 overexpressed transgenic mice and experimental animals:

8-10 weeks old B6C3 wild type male mice were purchased from (Charles River, Canada) to generate the transgenic mouse line SLMAP3-TM2 transgenic (TG) mouse line which was already established in the lab using the alpha-myosin heavy chain (α -MHC) promoter for cardiac specific expression in postnatal hearts was utilized in this study. The overexpressed SLMAP3-TM2 was speculated to homodimer with the endogenous SLMAP by its leucine zipper motifs (LZ) and potentially interferes with its cellular activity/targeting.

Animal care and experimental procedures were maintained according to the Guide for Care and Use of Laboratory Animals which were approved by Institutional Care Committee of the University of Ottawa. All mice were housed and kept in maintained environment, with a 12 hour light/12 hour dark cycle at room temperature of 22-23°C. Mice were freely allowed to access food and water at the animal facility.

2.2 Genotyping:

The genomic DNA extracted from ear tags using Red Extract-N-Amp™ PCR (Sigma), catalogue number R4775. Transgenic mice were recognized by polymerase chain reaction (PCR) using forward primer; 5'-GAAAAGCCTATCGAAATCAAGTTG-3' corresponding to exon 18 sequences, and reverse primer; 5'-ACCTTCTTAAGCTCTTCTTGCAAAG-3' corresponding to exon 19 sequences of SLMAP3. This results in a variation in PCR products around ~372 between 6-myc-tagged SLMAP3-TM2 transgenic and the endogenous SLMAP3. The difference was visualized by ethidium bromide staining in 1.5% DNA agarose gel. Later, the gel is scanned by BioRad Gel Doc Imaging System and kept for reference in characterizing the transgenic mice

from WT. Further, the genotyping was confirmed in Western blot experiments by incubating protein PVDF membrane with anti-myc antibody, which recognizes only 6-myc tagged SLMAP3 transgenic protein.

2.3 MI mouse model and echocardiography:

MI model in this study was induced in 9 week old mice by permanent left anterior descending (LAD) coronary artery ligation in a surgery known as coronary artery ligation (CAL) surgery (Xiao et al., 2012). Briefly, mice were anaesthetized with 2% isoflurane, intubated and ventilated using a mouse ventilator (Harvard Apparatus GmbH, Germany). Left lateral thoracotomy at fourth intercostal space was performed, and the proximal LAD (just 2mm below left auricle) was ligated using a 6-0 silk suture. MI was confirmed at time of surgery by blanching of blood distal to the ligation site, anterior wall motion dysfunction, and later by ST-segment elevation, which was recorded by electrocardiogram (ECG). This surgery was able to give as of ~40-45% left ventricular MI. As a control for MI, mice underwent sham operation where mice went through the same procedures of MI mice without LAD ligation. (MI surgery was performed by Rick Seymore, Heart Institute).

4 weeks post MI or sham surgeries, cardiac function was assessed by echocardiography and the following parameters were obtained in the short axis view at midpapillary level: left ventricular end diastolic and end systolic chamber diameters (LVEDD, LVESD), left ventricular wall thickness in diastole and systole (LV WT;d and LV WT;s) and ejection fraction percent (%EF). High resolution trans-thoracic echocardiography (Visualsonics Vevo2100 system, Canada) equipped with MS-400 transducer (30 MHz) was used on anaesthetized mice (2% isoflurane) to record the left ventricular function. One B-mode video, and three M-mode pictures

were reported for each mouse heart. The three M-mode pictures were analyzed and averaged in order to get the left ventricular functional parameters for each mouse. The mice were euthanized after echocardiography for heart measurements and staining.

2.4 Experimental groups:

Transgenic and wild type mice randomly underwent MI or sham operation, and divided into 3 groups: Wild type MI (WT MI), SLMAP3 transgenic MI (TG MI) and Sham control, which was mainly wild type mice. Each group has 6-22 mice were subjected to specific experiments.

2.5 Terminal deoxynucleotidyl-transferase-mediated dUTP nick end labeling (TUNEL) assay:

Apoptosis begins in first few hours post MI, and it reaches the maximum levels at 24-48 hours (Cheng et al., 1996). In addition, apoptosis is mainly localized at the margin of infarct area (Cheng et al., 1996; Olivetti et al., 1996). Thus, here in my experiment, 24 hour post MI, hearts were harvested, washed with phosphate buffered saline (PBS), fixed in 10% neutral-buffered formalin for 48 hours and then embedded in paraffin for sectioning. Four μm thickness cross sections were obtained from left ventricle just distal to the ligation site toward the remote area, and stained with TUNEL according to the manufacturer's instructions (Apop Tag® Plus Peroxidase In Situ Apoptosis Detection Kit, S7101, Millipore, USA). In brief, slides were deparaffinized in xylene bath, rehydrated through graded ethanol baths (100%-95%-70%) respectively and washed with PBS. After that, slides were pretreated with the freshly diluted Proteinase K to expose the antigen epitope, and then quenched in 3% hydrogen peroxidase to block the activity of endogenous peroxidases. After that, slides were incubated with equilibration

buffer and TdT enzyme for (10 seconds, 1 hour) respectively in humidified chamber at room temperature. The later reaction finished by Stop/Wash buffer, and then the slides were incubated for 30 minutes with working strength Anti-Digoxigenin conjugate at room temperature. Finally, the color developed with 3,3-diaminobenzidine (DAB) for ~4 minutes, and counterstained with methyl green stain. A negative control reagent lacks to the TdT enzyme was used to check the specificity of the reaction. Slides washed 3 times with PBS between in each step. The number of apoptotic cells in five different hot spots per 500 normal cells was measured and analyzed, which represents the apoptotic index.

2.6 Masson's trichrome staining:

Fibrosis is well-known mechanism in post MI, and because the fibrotic scar becomes well established at 4-6 weeks in post MI (Rubin et al., 2005). Thus, in my experiment, after MI by 4 weeks, the hearts were harvested, perfused through thoracic aorta with 15% potassium chloride (KCL) to get hearts arrested in diastolic phase, washed with PBS and then perfused and fixed in commercial 10% formalin for 48 hours. Four serial paraffin embedded sections, each 4 μ m thickness were obtained from each heart starting from the stitch site going distally toward the infarcted area in the following ordination (#1, #20, #40 and #55). These sections were stained with Masson's Trichrome (Thermo-scientific, Canada). The collagen in infarcted area stained blue, while the viable tissue stained red. Each section was scanned by Carl Zeiss Microimaging system (07740 Jena, Germany). Infarct size was measured in each section of each heart and averaged, which represents the length of scar (blue) to the total left ventricular length. Also, the collagen density was measured using ImageJ software, version 4.7 (NIH, USA). For mice surviving after 1 year post MI, longitudinal cardiac sections were obtained following similar processing steps as mentioned above in fibrosis, and stained with Masson's trichrome as well as

Hematoxylin and Eosin (H&E) stains to assess the morphology of infarct and to explore why these SLMAP3 TG mice survived and were better equipped than WT.

2.7 Immunohistochemistry

4 weeks post MI, hearts were harvested and treated in the same way as of Masson's trichrome steps. 4 μm cross section obtained from each heart post MI was stained with galectin3 following immunohistochemistry Biolegend protocol for paraffin-embedded sections. Briefly, slides were deparaffinized in xylene bath, rehydrated in ethanol series (100%-95%-70%-50%) respectively. Blocking of endogenous peroxidase by 3% hydrogen peroxide was done, followed by antigen retrieval step to expose the antigen epitope using (10 mM citrate buffer, pH 6.0) at 95-100°C for 10 minutes. After that, sections were blocked with 5% bovine serum albumin (BSA) in PBS to block any unspecific binding, and incubated with diluted primary antibody Galectin3 (1:2000, Abcam) overnight at 4°C. After serial washing of sections with PBS, the corresponding diluted horseradish peroxidase secondary antibody HRP (1:750, Jackson Immuno Research Laboratories Inc) was applied for one hour at room temperature. Finally, the color was developed with freshly made DAB, and counterstained with Fisher's hematoxylin dye.

2.8 Western blotting:

48 hours post MI, hearts were harvested, evacuated from blood and left ventricle (LV) and interventricular septum (IVS) dissected from the remaining heart using dissecting microscope. Further in MI's hearts, LV was dissected into three areas; infarcted (I), border (B) and remote (R) based on color of the myocardium and wall thickness. Directly, samples kept in liquid nitrogen and then frozen in -80°C till the time of experiment. Each area of LV was lysed with cell lysis buffer (CST) containing 20 mM Tris-Hcl (pH7.5), 150 mM NaCl, 1mM

Na₂EDTA, 1mM EGTA, 1% Triton, 2.5 mM sodium pyrophosphate, 1mM β-glycerophosphate, 1mM Na VO₄ and 1μg/ml leupeptin for total protein extraction. Protein concentrations were measured using bicinchoninic acid protein kit (Pierce BCA Protein Assay Kit, Thermo Scientific, USA). 30-40 μg protein lysates in equal amounts were loaded, separated via 12% sodium dodecylsulfate polyacrylamide gel electrophoresis (SDS-PAGE) and transferred onto polyvinylidene difluoride membrane (PVDF, Merck Millipore, Billerica, MA, USA) overnight at 4°C. After blocking in 5% nonfat milk or 5% BSA in TBST for 1 hour, membranes were incubated in anti-Bax antibody (1:1000, Cell Signaling Technology), anti-Caspase3 antibody (1:1000, Cell Signaling Technology), anti-Bcl2 antibody (1:500, Santa Cruz), anti-Caveolin3 antibody (1:25000, Abcam), anti-αTubulin antibody (1:10000, Cell Signaling Technology), anti-SLMAP antibody (1:1000, Abnova), anti-Myc antibody (1:1000, Sigma Aldrich), anti-phospho-ERK 44/42 antibody (Thr202/Tyr204, 1:5000, Cell Signaling Technology), anti-total pERK 44/42 antibody (P44/42 ERK1/2, 1:1000, Cell Signaling Technology), anti-Galectin3 antibody (1:1000, Abcam) and anti-GAPDH antibody (1:10000, Thermo Scientific) overnight at 4°C. Membranes were rinsed for at least three times in TBST buffer for 30 minutes and subsequently incubated with the corresponding HRP secondary antibody (1:10000, Jackson Immuno Research Laboratories Inc) for one hour at room temperature. Finally, blots were developed into Autoradiography Film (Denville Scientific Inc) using enhanced chemiluminescence detection substrate (Roche Diagnostic GmbH, Germany). Protein densitometric values were quantified and normalized to the loading control protein using Image Lab software version 4.0 (Bio-Rad Laboratories Inc, Canada).

2.9 Other parameters:

Heart weight, lung weight, heart weight to body weight (HW:BW) ratio and lung weight to body weight (LW:BW) ratio were measured and documented in this study.

2.10 Statistical analysis:

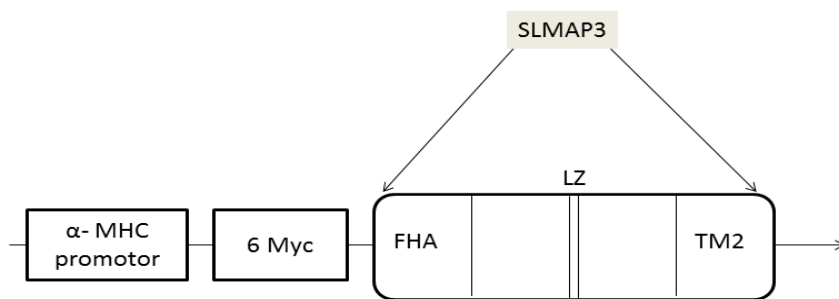
All data are presented as mean \pm SEM. Normally distributed quantitative data were analyzed using One Way ANOVA for multiple group comparison, followed by post hoc Bonferroni's test to compare multiple groups to each other. Survival-death curve was analyzed using Kaplan-Meier method. All analysis was performed using Graph Prism software version 5.0. Probability value (p value) <0.05 was considered to be statistically significant.

CHAPTER 3: RESULTS

3.1 *Generation of SLMAP3-TM2 transgenic mice:*

Previous SLMAP3-TM2 transgenic mouse model was generated in our lab. The SLMAP3 construct encompassed the specific forkhead-associated domain (FHA), encoded by exon I, coiled coil two leucine zippers, encoded by exon III and IV respectively, as well as transmembrane domain 2 (TM2), encoded by XXIV (figure 2A). Three different expressers of SLMAP3 were generated (high, medium, and low) as shown in figure 2B. In my current study, I worked on the high expresser of SLMAP3 in order to see a reasonably prominent phenotype.

A.



B.

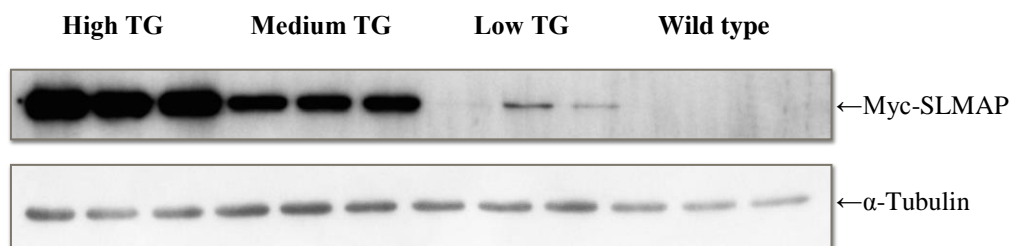


Figure 2: Generation of SLMAP3-TM2 transgenic mice. A) The SLMAP3-TM2 construct.

SLMAP3 gene was targeted specifically to postnatal hearts using alpha-myosin heavy chain (α -MHC) promotor, and tagged with 6-myc epitope in order to track it within cardiac cells.

SLMAP3 construct composed of forkhead-associated domain, two leucine zipper motifs, carboxyl terminal transmembrane domain (TM2), which is responsible for SLMAP targeting to subcellular compartments. These mice lines were generated by Maysoon Salih B).

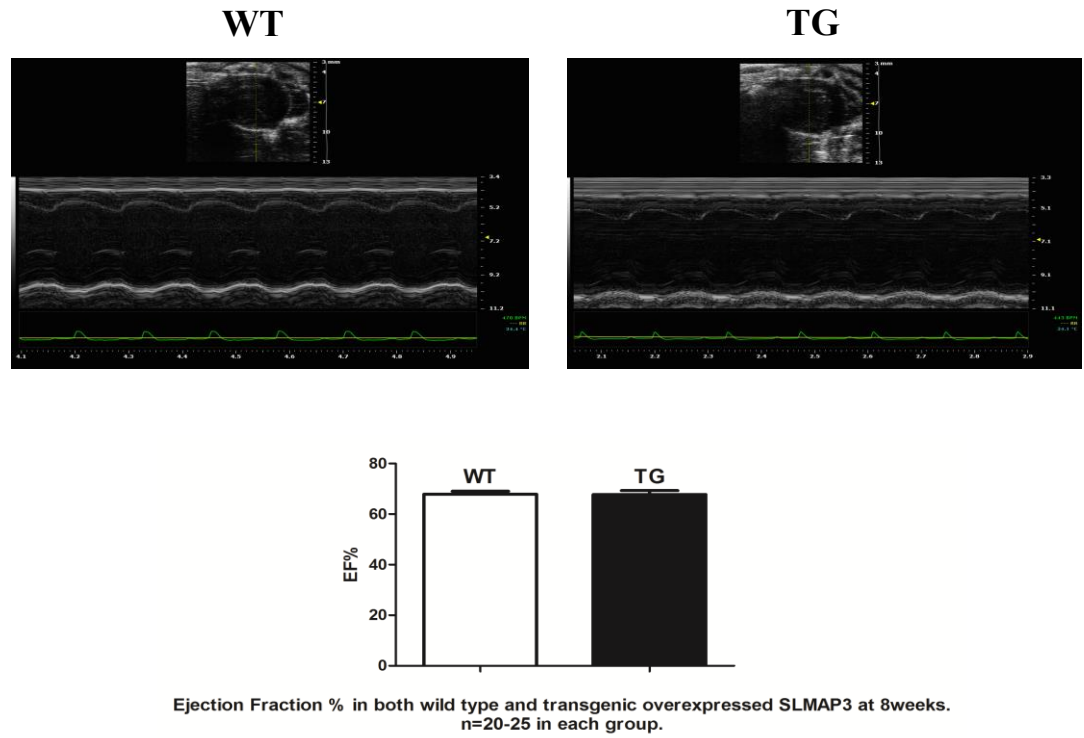
Representative Western blots for myc-SLMAP3 expression in transgenic mice cardiac lysates in 5 weeks. A mouse lines carrying different copies of the transgene (low, medium and high) were assessed for SLMAP expression. Western blot analysis was done on mouse heart tissue to confirm the presence of the different levels of myc-SLMAP3 present in these mice by incubating with myc antibody. Consistent with the transgene data the high expresser had significantly higher

myc-SLMAP3 protein levels compared to the medium and low expressers while non TG mice had no detectable six-myc.

3.2 *Baseline cardiac phenotype and histology:*

SLMAP3 transgenic mice lines with high expression were employed in the following studies. The TG mice did not show any difference in term of function, survival and histological changes compared to wild type (WT) littermates. Echocardiography analysis of these SLMAP3 TG mice at 8 weeks of age has shown as normal cardiac phenotype as those seen in the corresponding WT littermates. Cardiac function was expressed in ejection fraction percent (%EF), which was ($66\% \pm 7.42$, $67\% \pm 9.36$, $p < 0.05$) in SLMAP3 TG and WT mice respectively (figure 3A). Furthermore, histological analysis of myocardium stained with hematoxylin and eosin (H&E) showed no difference in morphological features of SLMAP3 TG hearts, no hypertrophy or dilatation, and no distortion in cardiomyocytes were seen in these hearts compared to WT littermate (figure 3B).

A.



B.

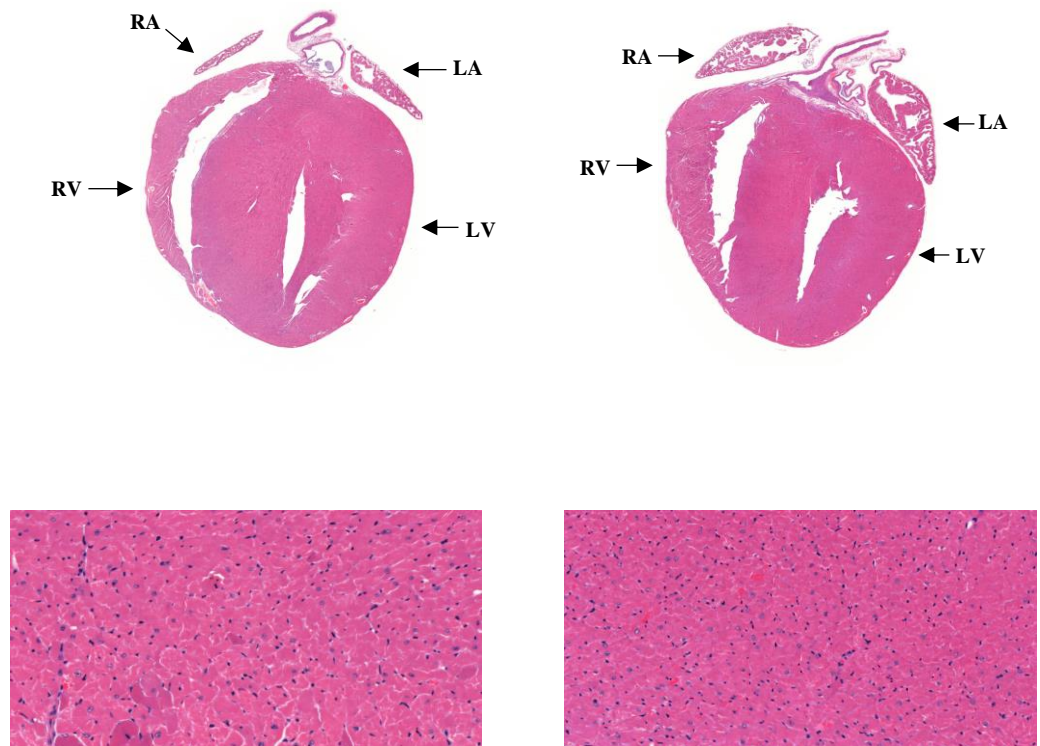


Figure 3: Cardiac phenotype of SLMAP3 TG mice. A). Baseline echocardiography analysis.

Representative M-mode echocardiography in 8 week old mouse heart were analyzed and left ventricular functional analysis was represented as ejection fraction percent (%EF); amount of blood ejected from the left ventricle during systole, which is normally $\sim 70\% \pm 8.68$ (Lu et al., 2016). Here, the results showed the left ventricular ejection fraction (%EF) at $\sim 66\% \pm 7.42$ in SLMAP3 TG mice compared to $\sim 67\% \pm 9.36$ in WT littermates, leading to the conclusion that these TG mice have as normal LV function as WT ($p < 0.05$). B). *Histology in 16 week old SLMAP3 TG heart with H&E staining.* Whole heart amounts in upper row (bar=1000 μ m) elucidate that there is no gross changes in structure (RA= right atrium, LA= left atrium, RV= right ventricle, LV= left ventricle) in SLMAP3 TG heart compared to WT. The lower row (bar=100 μ m) indicates no obvious changes in cardiomyocyte representation in SLMAP3 transgenic mouse heart sections leading us to believe that overexpressed SLMAP3 in TG myocardium results in no cardiac defects or malformations.

3.3 Cardiac function 4 weeks post MI was preserved by SLMAP3 overexpression:

A total of 45 mice randomly underwent CAL and sham operations; 10 were sham controls, 19 were WT MI and 16 were SLMAP3 TG MI. Four weeks post MI, echocardiography was carried out for each mouse survived post MI (10 shams, 15 WT MI and 16 SLMAP3 TG MI). Echocardiography showed that WT MI mice exhibited more adverse cardiac dysfunctions in both systole and diastole as documented by (%EF, 36.4 ± 15.25 vs. 49.2 ± 17.02 , $p < 0.05$) in comparison with SLMAP3 TG MI group (Table 1, figure 4). This deterioration in cardiac function was associated with more LV dilation in WT MI as expressed in left ventricular end diastolic diameters and left ventricular end systolic diameters (LVEDD, 4.54 ± 0.113 vs. 4.12 ± 0.096 ; LVESD, 3.59 ± 0.087 vs. 3.02 ± 0.094) respectively (Table 1, figure 4). Furthermore, greater LV wall thinning was notable in WT MI in both diastole and systole as expressed in left ventricular wall thicknesses (LV WT;d, 0.59 ± 0.030 vs. 0.64 ± 0.027 ; LV WT;s, 0.076 ± 0.041 vs. 0.88 ± 0.038) in comparison to SLMAP3 TG MI group (Table 1). The ratio lung weight to body weight (LW:BW) was higher in WT MI hearts (0.64 ± 0.02 vs. 0.57 ± 0.013) in comparison to SLMAP3 TG MI group, while the ratio of heart weight to body weight (HW:BW) was not different between the two groups of MI (0.44 ± 0.015 vs. 0.45 ± 0.021) (Table 1).

In summary, as expected, adverse cardiac dysfunction was observed in both MI groups in comparison to sham control ($p < 0.05$), which was expressed in echocardiography parameters, but surprisingly the cardiac contractility of SLMAP3 hearts was preserved up to ~50% (%EF, $p < 0.05$) concomitant with less cardiac dilation in both diastole and systole (LVEDD, LVESD, LV WT;d, LV WT;S, and LW:BW) compared to WT.

Table 1: *Functional analysis 4 weeks post MI.* The represented data were means of three separate M-mode measurements. WT MI: wild type myocardial infarction; TG MI: transgenic myocardial infarction; BW: body weight; HW: heart weight; LW: lung weight; HR: heart rate; LVEDD: left ventricular end diastolic diameter; LVESD: left ventricular end systolic diameter; LV WT;d: left ventricular wall thickness in diastole; LV WT;s: left ventricular wall thickness in systole; %EF: ejection fraction percent. Anova Test was used for significance analysis in both WT MI and TG MI vs. sham control.

Parameter	Sham group (n=10)	WT MI (n=15)	TG MI (n=16)	Anova Test vs. Sham
BW (g)	34.8±1.68	33.33±1.67	35.11±1.73	ns
HW (g)	0.126±0.007	0.146±0.008	0.161±0.009	<0.05
LW (g)	0.170±0.005	0.212±0.002	0.201±0.004	<0.05
HW:BW (%)	0.37±0.027	0.44±0.015	0.45±0.021	<0.01
LW:BW (%)	0.50±0.028	0.64±0.02	0.57±0.013	<0.01
HR (beat/min)	428±15.35	478.5±19.21	469±11.71	<0.01
LVEDD (mm)	3.44±0.090	4.54±0.113	4.12±0.096	<0.001
LVESD (mm)	1.81±0.069	3.59±0.087	3.02±0.094	<0.001
LV WT;d (mm)	0.90±0.033	0.59±0.030	0.64±0.027	<0.001
LV WT;s (mm)	1.34±0.046	0.76±0.041	0.88±0.038	<0.001
%EF	67.5±10.78	36.4±15.25	49.2±17.02	<0.0001

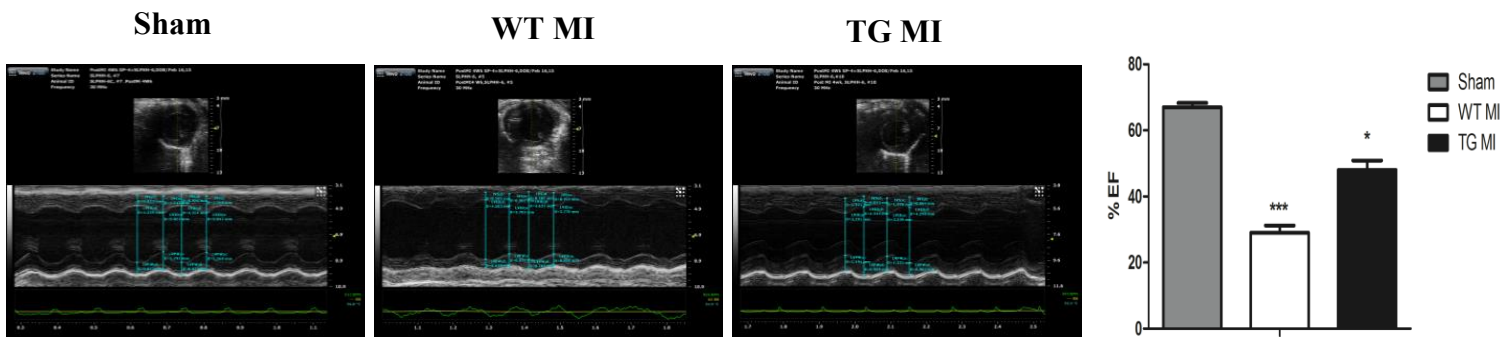


Figure 4: *Echocardiography of 13 week old mice post MI.* Representative M-mode echocardiography images 4 weeks post MI showed a significant reduction in ejection fraction percent (%EF) in MI groups compared to sham (p<0.0001), but this reduction was significantly

greater in WT MI (%EF~36.4%±15.25) relative to TG MI (%EF~49.2%±17.02), $p<0.05$. Left ventricular dilatation associated with reduced wall thickness were observed in MI groups in both systole and diastole compared to sham ($p<0.001$), which was represented in (LVEDD;d, LVESD;s, LV WT;d and LV WT;s) respectively. Tissues were harvested and weighed after echocardiography (Table 1). The ratio HW:BW and the ratio LW:BW were significantly greater ($p<0.01$) in MI groups in comparison with sham indicating development of heart failure in those mice. LW:BW ratio was notably reduced in TG MI group compared to WT MI, which was close to significance ($p=0.07$), but there was no difference in HW:BW ratio between two groups of MI ($p>0.05$). n=10 in sham group, n= 19 in WT MI group, n= 16 in TG MI group.

3.4 Kaplan Meier curve of SLMAP3 TG mice post MI:

35 mice randomly underwent MI operation, 18 were WT MI mice, 17 were SLMAP3 TG MI while 10 were sham controls. These mice were monitored for survival and death over 12 months (Kaplan Meier curve for probability of death). 70% of wild type mice died, while no death was recorded in SLMAP3 TG mice post MI ($p < 0.01$) (figure 5). Early deaths in the first week post MI were mainly due to rupture of myocardium, while later deaths were mainly due to heart failure.

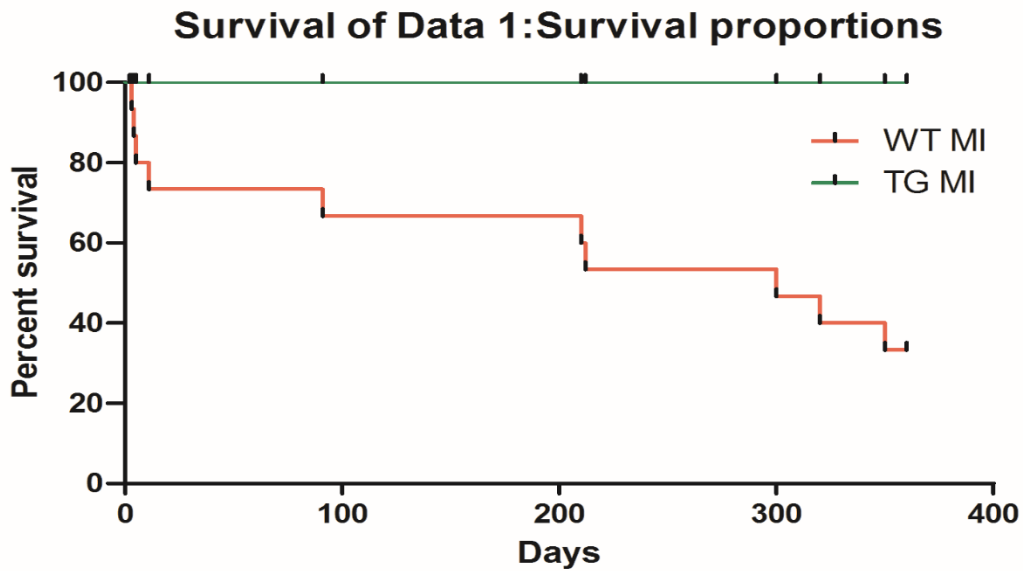


Figure 5: Kaplan Meier curve in SLMAP3 TG post MI. 35 mice randomly underwent MI operation, 18 were WT MI mice and 17 were TG MI. Additionally, ten mice were a sham control group. These mice were monitored for survival and death over 12 months. 13 WT mice out of 18 (70%) died, while no death was recorded in SLMAP3 TG mice post MI ($p < 0.01$).

3.5 *Heart failure biomarker galectin3 was markedly reduced in SLMAP3 hearts:*

Many biological markers nowadays are used to explore development of heart failure in post MI such as galectin3 (Sharma et al., 2004). Galectin3 is one of the recent and powerful diagnostic tools to assess development of heart failure as well as to predict its severity (Leone & Iacoviello, 2015). In my project, expression level of galectin3 was significantly increased in MI heart lysates in comparison with sham as assessed by Western blot analysis. Surprisingly, galectin3 expression was markedly attenuated in SLMAP3 TG MI ($p < 0.01$) in comparison with WT MI (Figure 6A). Moreover, this result was supported by galectin3 immunohistochemistry (IHC), since less galectin3 positive stained area was observed in SLMAP3TG myocardium post MI compared to WT (Figure 6B).

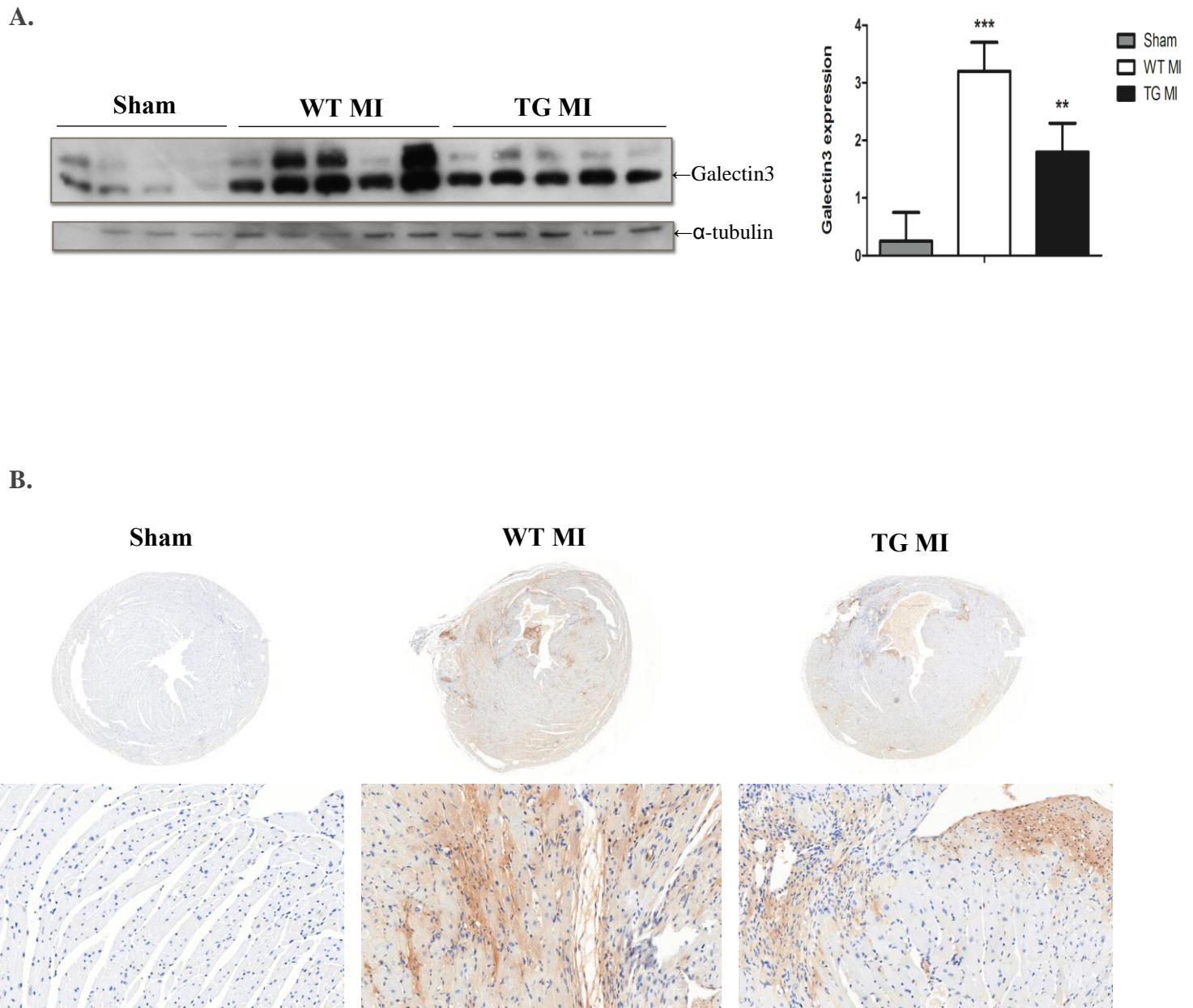


Figure 6: Heart failure biomarker “galectin3” expression in *SLMAP3* TG hearts post MI. A). *Representative Western blot for galectin3 expression:* The heart failure biomarker galectin3 expression was markedly upregulated in both groups of MI compared to sham control ($p < 0.0001$), but this expression was markedly attenuated in TG MI (1.8 ± 0.20) in comparison to WT MI (3.2 ± 0.35), $p < 0.01$, $n = 4-5$ in each group. B). *Staining with galectin3 indicates a higher incidence of heart failure in WT MI by immunohistochemistry:* 4 week post MI cross sections (in

13 week old mouse heart) were stained with galectin3 (in brown color), and counterstained with hematoxylin (in purple). IHC stains showed galectin3 was present in MI hearts compared to sham; however, there was a much higher presence of galectin3 in WT MI myocardium relative to TG MI.

3.6 Collagen levels and infarct size were reduced by SLMAP3 in post MI:

Scar formation following MI is an eventual fate, which becomes well established at 4-6 weeks post MI (Rubin et al., 2005). In order to assess the mature scar, 4 weeks post MI cross sections were stained with Masson's Trichrome, in which fibrotic tissue stained in blue, while viable myocardium stained in red. Fibrosis was significantly notable post MI in comparison with sham ($p < 0.0001$) (figure 7, upper row). However, infarct size as well as collagen levels were significantly reduced in SLMAP3 TG myocardium ($p < 0.05$, $n = 20-22$ in each MI group, $n = 5$ in sham control) in comparison to WT (figure 7, upper & lower rows).

Later after 1 year post MI, the mice which survived MI were sacrificed, and their hearts explored in order to assess any morphological difference between SLMAP3 TG hearts and WT. All the remaining WT hearts had a pathognomonic balloon dilated, pale (? avascular) myocardium at the site of infarct, which gave the heart asymmetrical appearance. While SLMAP3 TG hearts had notable symmetrical global appearance and the infarct site was rather red (? vascular), suggesting growing of new viable tissue at the infarct site. Furthermore, longitudinal cardiac sections obtained from those hearts and stained after processing with Masson's trichrome. Thin rim of fibrotic tissues were obviously seen in left ventricular walls of WT hearts at the infarct site, while more viable and thicker left ventricular walls were seen in SLMAP3 TG hearts at infarct site (figure 8).

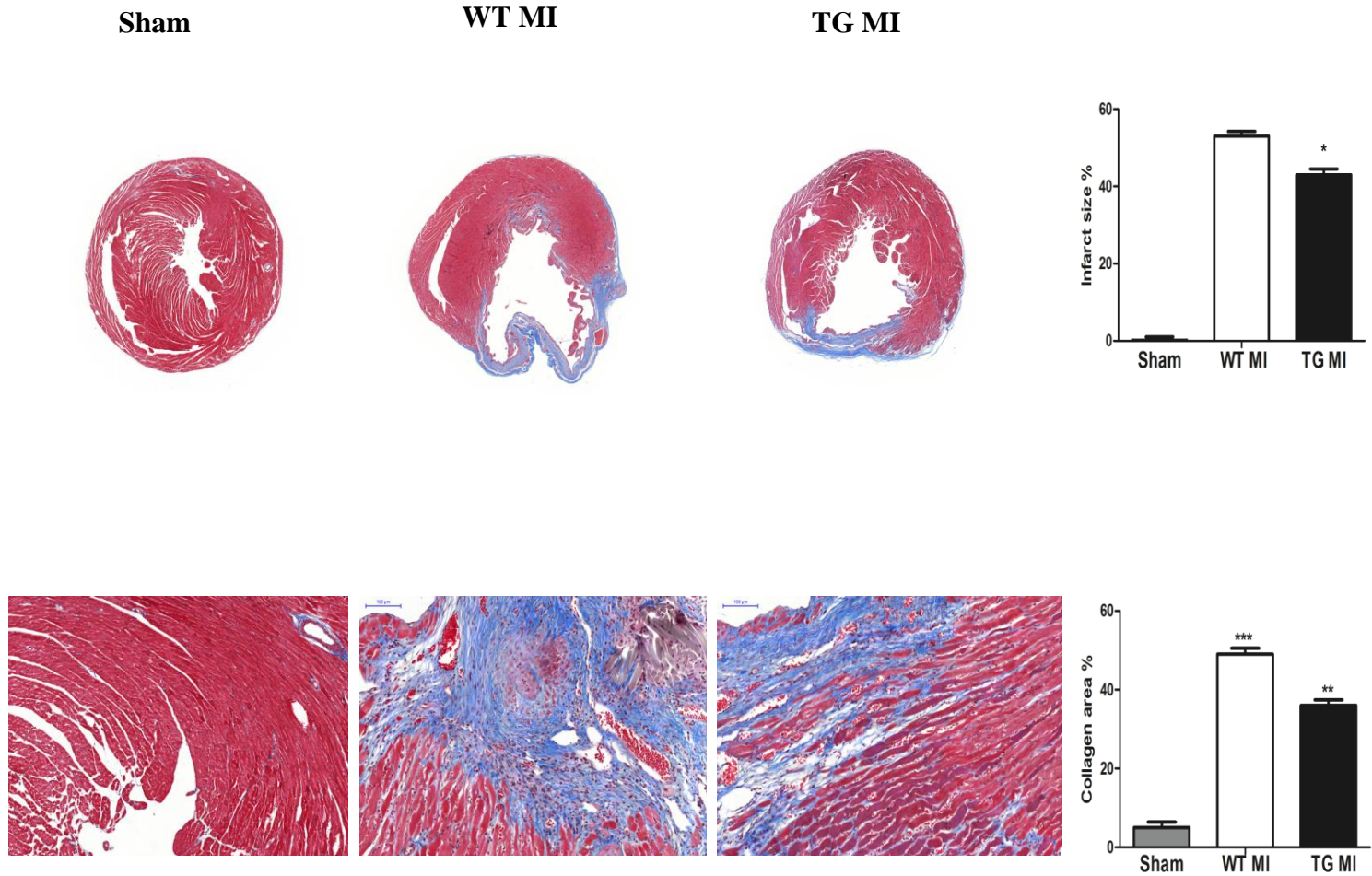


Figure 7: Cardiac fibrosis and infarct size in *SLMAP3* TG myocardium post MI. A) Viable myocardium (red), while fibrosis (blue) was investigated by using Masson's trichrome staining. In sham operated control group sections, no fibrosis was observed. In contrast, blue scar tissues could be easily observed in the infarct zone of MI group sections ($p < 0.0001$). Four cross sections of each heart were stained with M.T and analyzed for infarct size percent and collagen area percent, bar=1000 μm in upper row, bar=100 μm in lower row. The represented infarct size (upper row) and collagen area (lower row) were significantly higher in WT MI myocardium (IS~53±9.30, CA~47±7.37) in comparison to TG MI myocardium (IS~43±8.82, CA~35±5.15), $p < 0.05$.

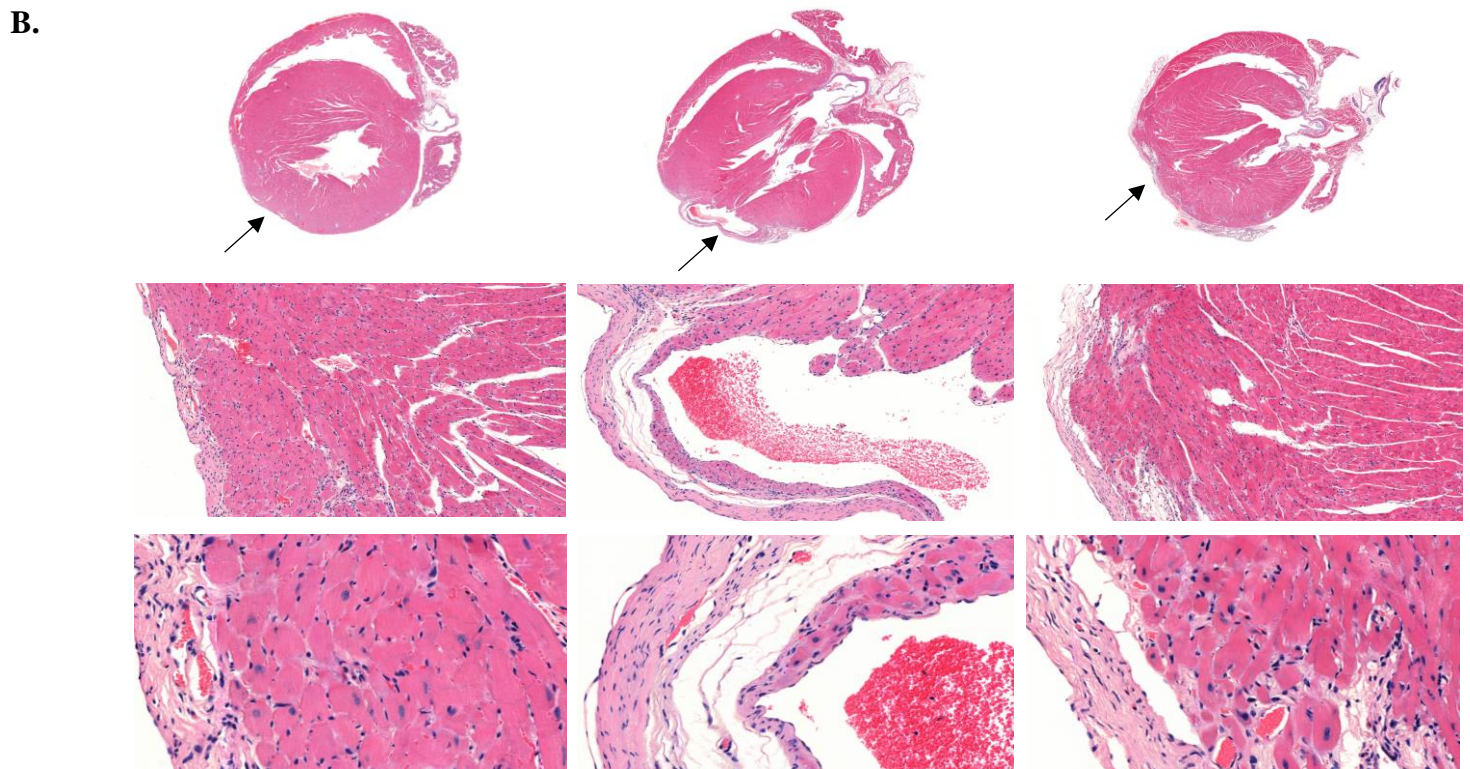
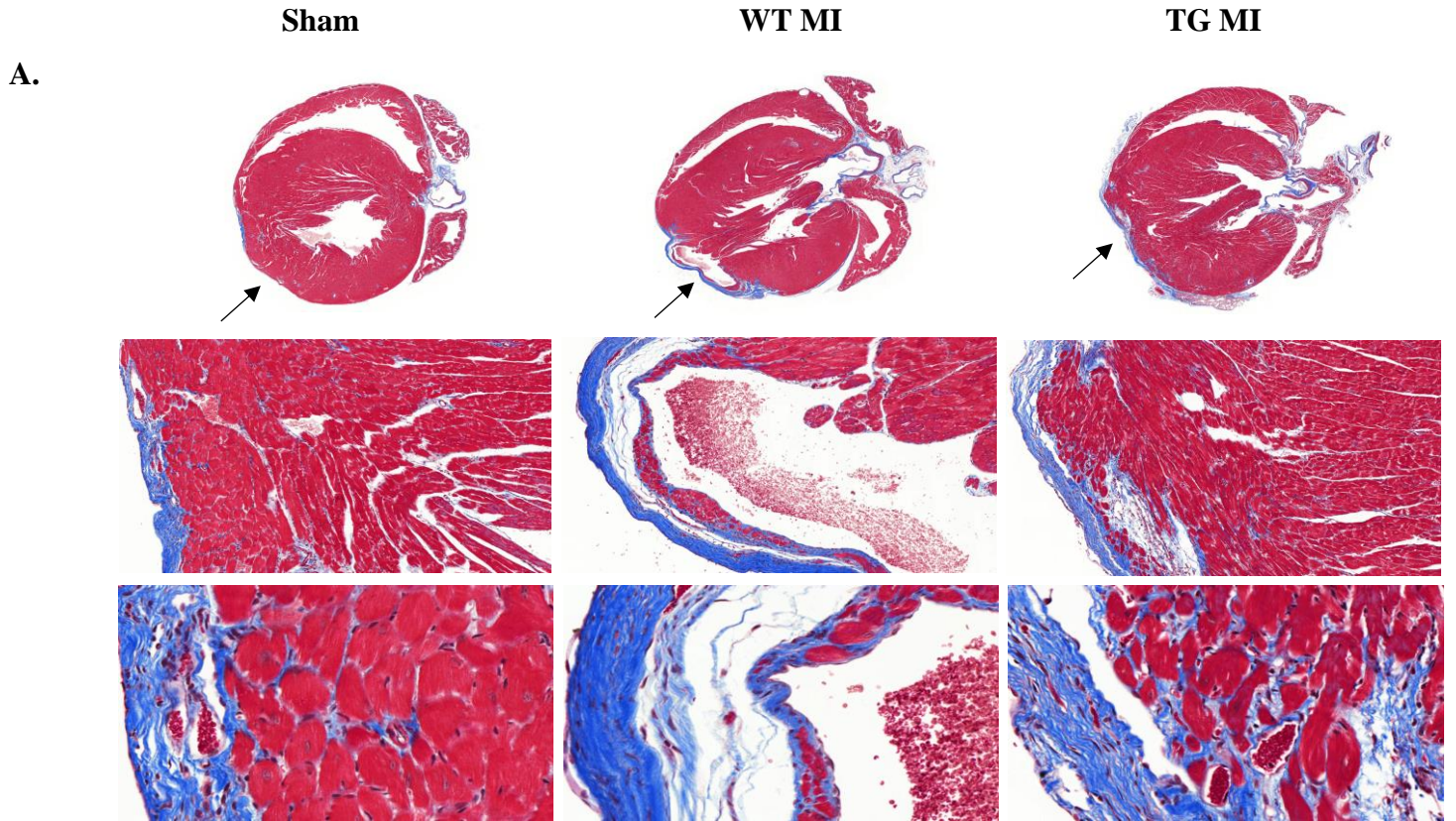


Figure 8: *Histology of mouse myocardium 1 year post MI.* A) *Masson's trichrome staining 1 year post MI:* Longitudinal cardiac section of WT myocardium stained with Masson's trichrome shows dilated and thinner left ventricular wall with dense scar tissue at the infarct area. A thicker left ventricular wall are notable with less fibrotic tissue as well as more viable tissue in SLMAP3 TG myocardium at the infarct site, bar=2000 μm in upper row, bar=200 μm in middle row, and bar=50 in lower row. B) *Hematoxylin and Eosin staining (H&E):* Longitudinal cardiac sections show the infarct as well as the border area of SLMAP3 myocardium with notably more blood vessels and cardiomyocytes in comparison with WT, bar=2000 μm in upper row, bar=200 μm in middle row, and bar=50 in lower row. N.B. Arrow indicating to the apex of the heart, which is expected to be impacted by infarct in case of MI.

3.7 Apoptosis was attenuated in *SLMAP3* myocardium post MI:

In view of apoptosis and its relative contribution to development of cardiac remodeling (Kumar & Clark, 2009; Olivetti et al., 1996), TUNEL assay was performed to detect early apoptosis in 24 hours post MI since it is expected to be at its maximum magnitude (Cheng et al., 1996). As expected, the area of positive TUNEL nuclei was significantly abundant in MI myocardium ($p < 0.001$) compared to sham (Figure 9, upper row). Apoptotic index was measured and shown markedly reduced apoptotic index in *SLMAP3* TG myocardium ($p < 0.05$, $n = 20-22$ in each group) compared to WT MI (Figure 9, lower row).

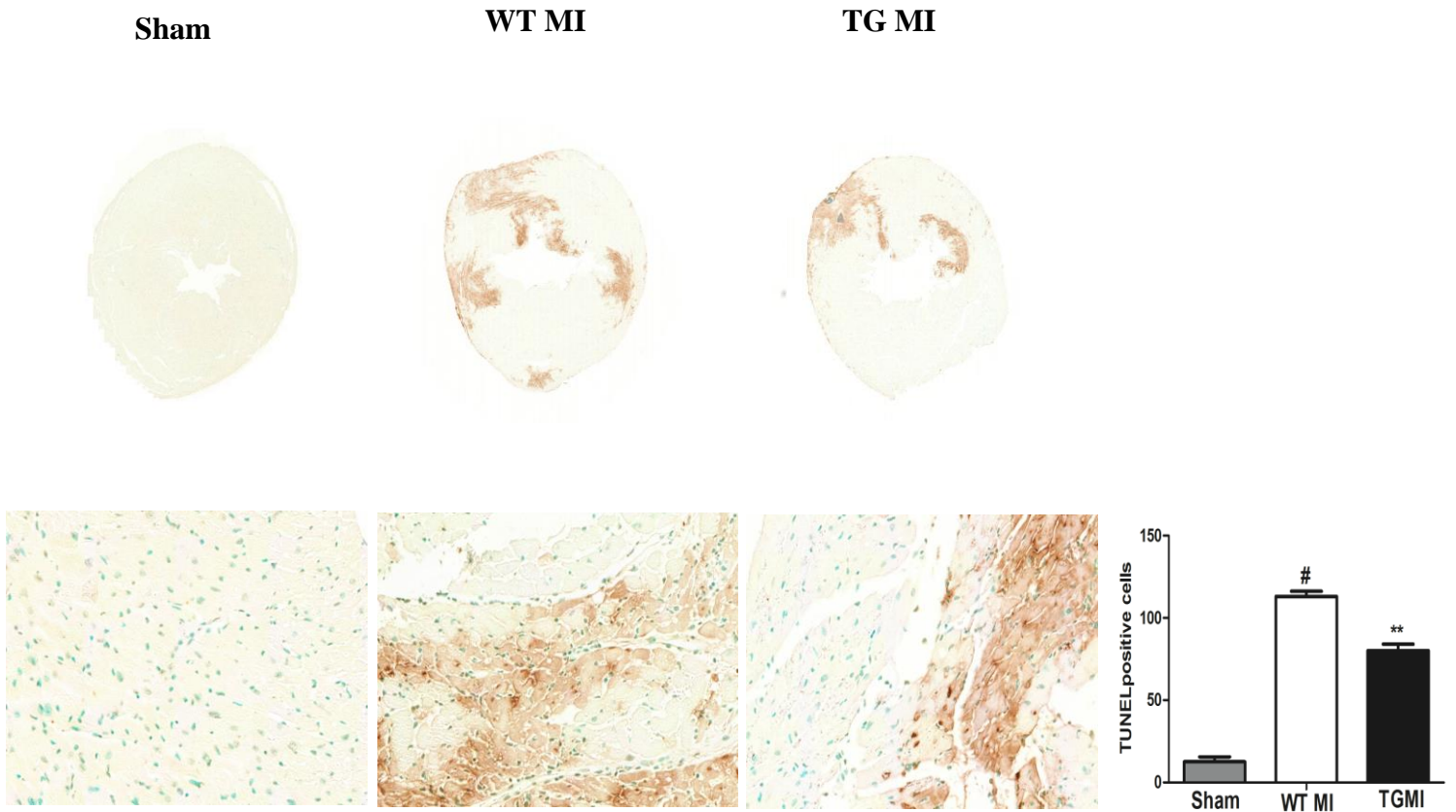


Figure 9: TUNEL assay of SLMAP3 TG myocardium post MI. Apoptotic cells that underwent extensive DNA fragmentation during late stages of apoptosis were stained in brown, while viable cells were counterstained with methylene green dye, bar=1000 μ m in upper row. Apoptotic index measured and was significantly higher in WT MI myocardium (112 ± 15.32) compared to TG MI myocardium (77 ± 11.48), $p < 0.05$, $n = 20-22$ in each group, bar=50 μ m in lower row.

3.8 *SLMAP3 reduced prodeath and enhanced prosurvival signals post MI.*

Endogenous SLMAPs levels (SLMAP3, SLMAP2 and SLMAP1) were elevated in post MI in the non-infarct remote area of left ventricle in WT MI in comparison to WT sham (figure 10). Furthermore, endogenous SLMAP3 level was notably upregulated in all areas of left ventricle post MI; Infarct (I), border (B), and remote (R) and the significance was ($p < 0.05$, $p = 0.08$, $p < 0.01$) respectively in comparison to sham (figure 11). This suggests that elevated levels of endogenous SLMAP3 in all areas of LV post MI might serve to modulate such a protective response. For this reason I looked up some proapoptotic and antiapoptotic proteins in SLMAP3 TG heart post MI. Expression levels of prodeath proteins (Bax and Caspase3) in all three areas of left ventricle post MI (I, B, R) were significantly upregulated in both MI groups compared to sham ($p < 0.001$) (figure 12a, 14a, 16a). Surprisingly, these proapoptotic proteins in these areas were markedly reduced in SLMAP3 TG post MI ($p < 0.001$) in comparison to WT MI (figure 12a, 14a, 16a). In contrast, prosurvival Bcl2 expression level post MI was significantly higher in SLMAP3 TG MI compared to WT MI ($p < 0.001$) (Figure 12a, 14a, 16a). Interestingly, apoptotic index was measured and expressed in the ratio of Bax:Bcl2 in all areas of LV post MI, which was remarkably less in SLMAP3 TG MI compared to WT MI ($p < 0.0001$) (Figure 12b, 14b, 16b).

In view of these data presented in SLMAP3 TG hearts post MI, it appears that increased expression of SLMAP3 in TG hearts may serve a protective response to the stress induced by MI throughout upregulation of proapoptotic protein (Bcl2), and downregulation of proapoptotic proteins (Bax, and caspase3).

3.9 *Cav3* expression was enhanced, while *ERK1/2* signaling mechanism of HF was depressed in *SLMAP3* TG mice in post MI:

In the current study, in all areas of left ventricle (I, B, R), the cardioprotective caveolin3 was significantly upregulated in *SLMAP3* transgenic hearts post MI ($p < 0.001$, $p < 0.001$, $p < 0.05$) respectively in comparison to WT (figure 13, 15, 17). In contrary, phospho-*ERK1/2* the well-known signal in pathological cardiac hypertrophy was downregulated in *SLMAP3* transgenic hearts in all areas of left ventricle (I; B; R) post MI ($p < 0.05$, $p < 0.05$); ($p < 0.05$, $p < 0.01$); ($p < 0.05$, $p < 0.01$) respectively compared to WT (figure 13, 15, 17).

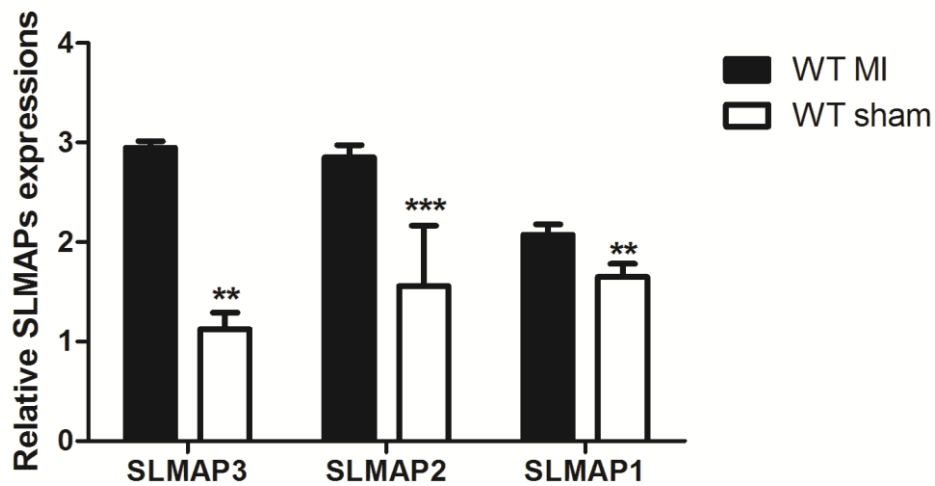
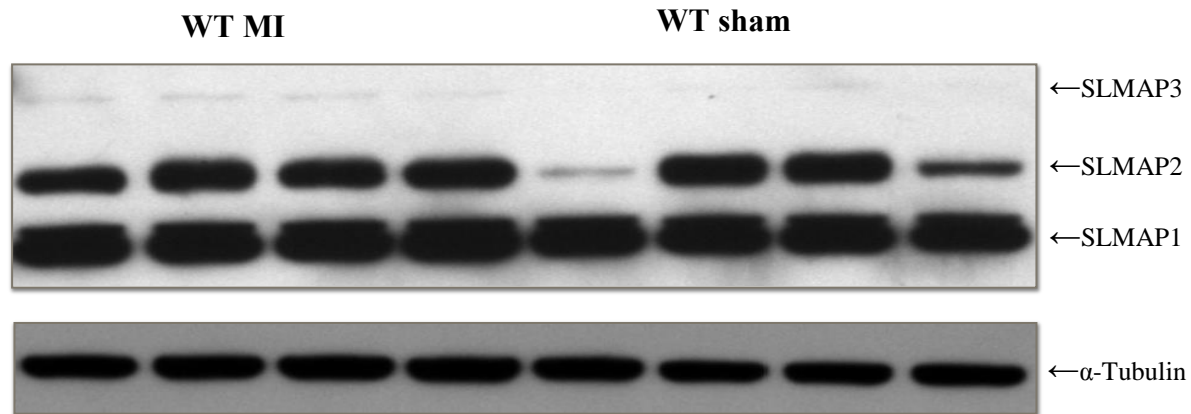


Figure 10: Expression of endogenous SLMAP isoforms in the remote area post MI. Western blot analysis of left ventricle lysates post MI shows significant upregulation of all isoforms of endogenous SLMAPs (SLMAP3, SLMAP2, and SLMAP1) at remote myocardium in WT MI in comparison with WT sham. $P < 0.05$, $n = 4$ in each group.

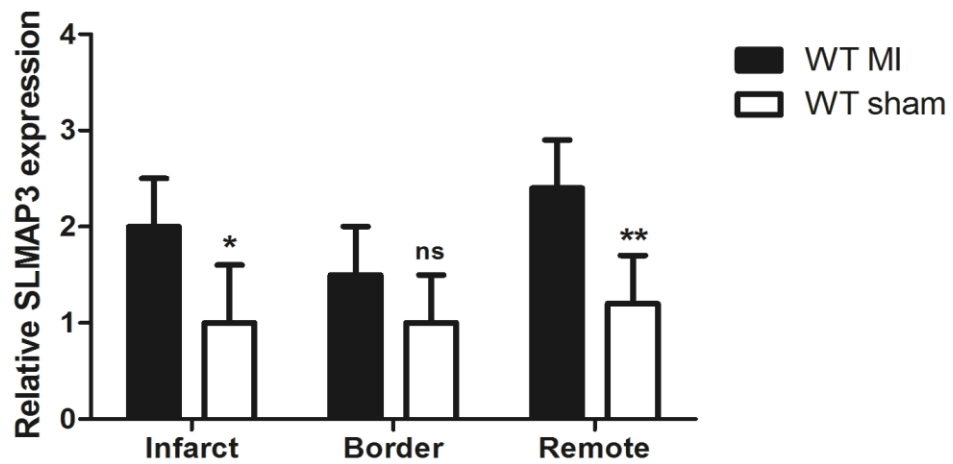
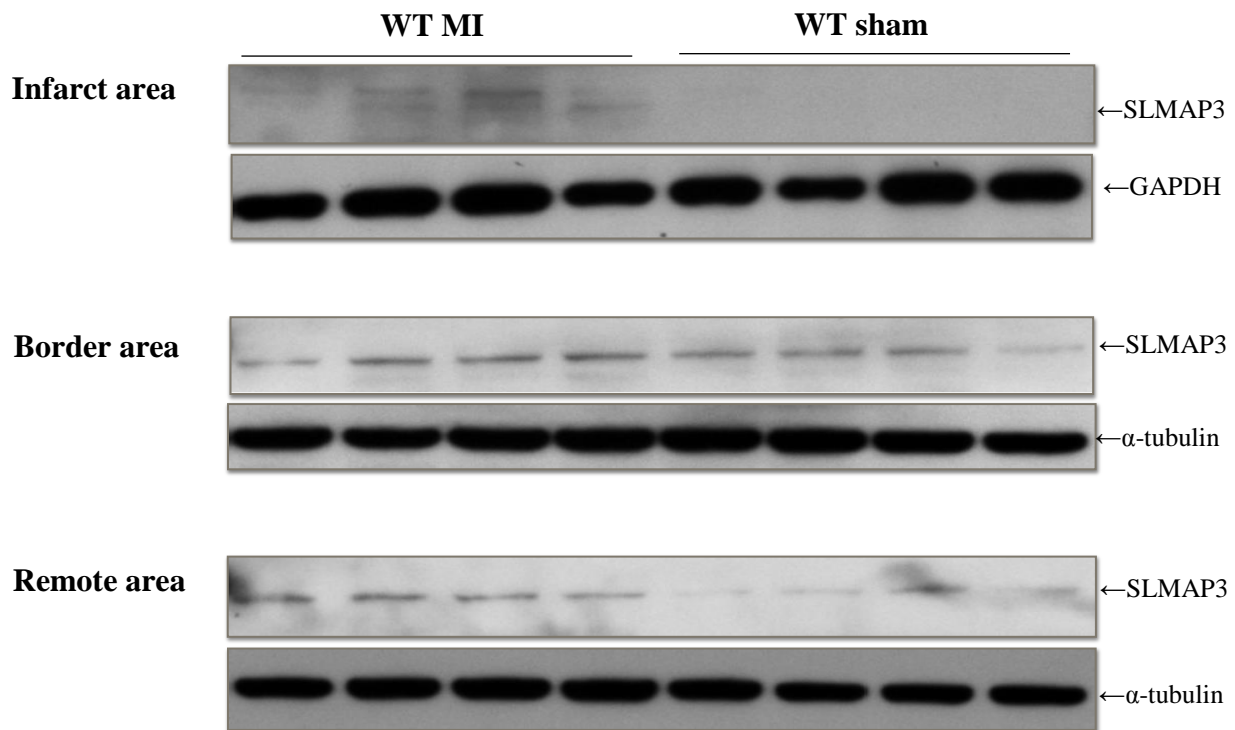
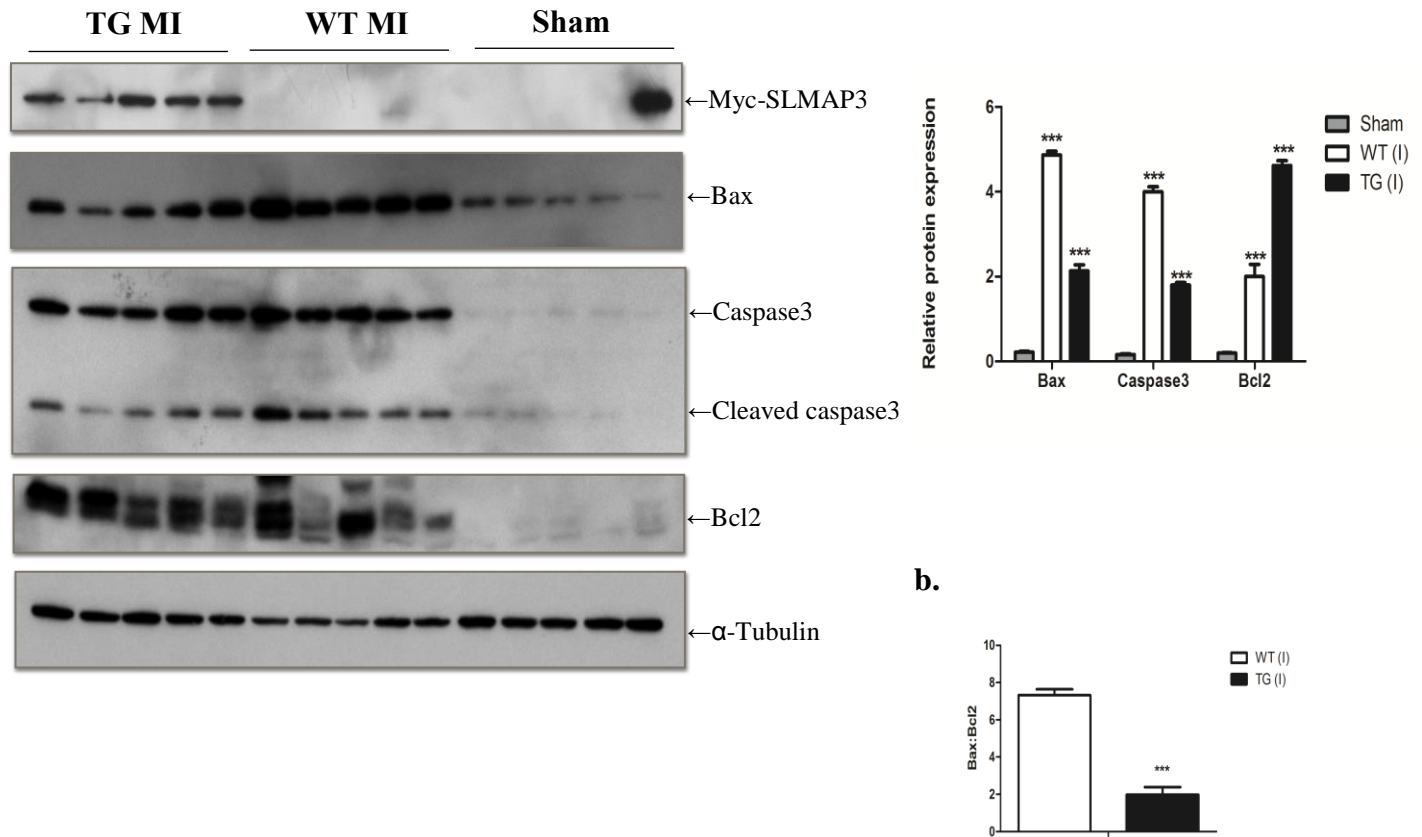


Figure 11: Expression of SLMAP3 protein in different areas of left ventricle (I, B, R) post MI.

Western blot analysis shows significant upregulation of endogenous SLMAP3 in left ventricular lysates of infarct (I) area as well as remote (R) area ($p < 0.05$, $p < 0.01$) respectively. In border area, endogenous SLMAP3 was notably elevated while p value wasn't significant, but it was close to significance ($p = 0.08$), $n = 4$ in each group.

Infarcted area (I)

a.



b.

Figure 12: Expression of proapoptotic and antiapoptotic proteins in infarct area (I) post MI. a)

Western blot analysis of infarct tissue post MI shows elevated levels of proapoptotic proteins (Bax & caspase3), as well as antiapoptotic protein Bcl2 in MI groups in comparison to sham

($p < 0.001$). Bax & caspase3 were markedly reduced in SLMAP3 TG MI ($p < 0.001$) compared to

WT MI. However, the antiapoptotic Bcl2 expression was significantly upregulated post MI in

SLMAP3 TG ($p < 0.001$) in comparison to WT. b) The ratio Bax:Bcl2 was measured, and shows a

great reduction in apoptotic index in SLMAP3 TG post MI ($p < 0.001$) compared to WT, $n = 4-5$ in

each group.

Infarcted area (I)

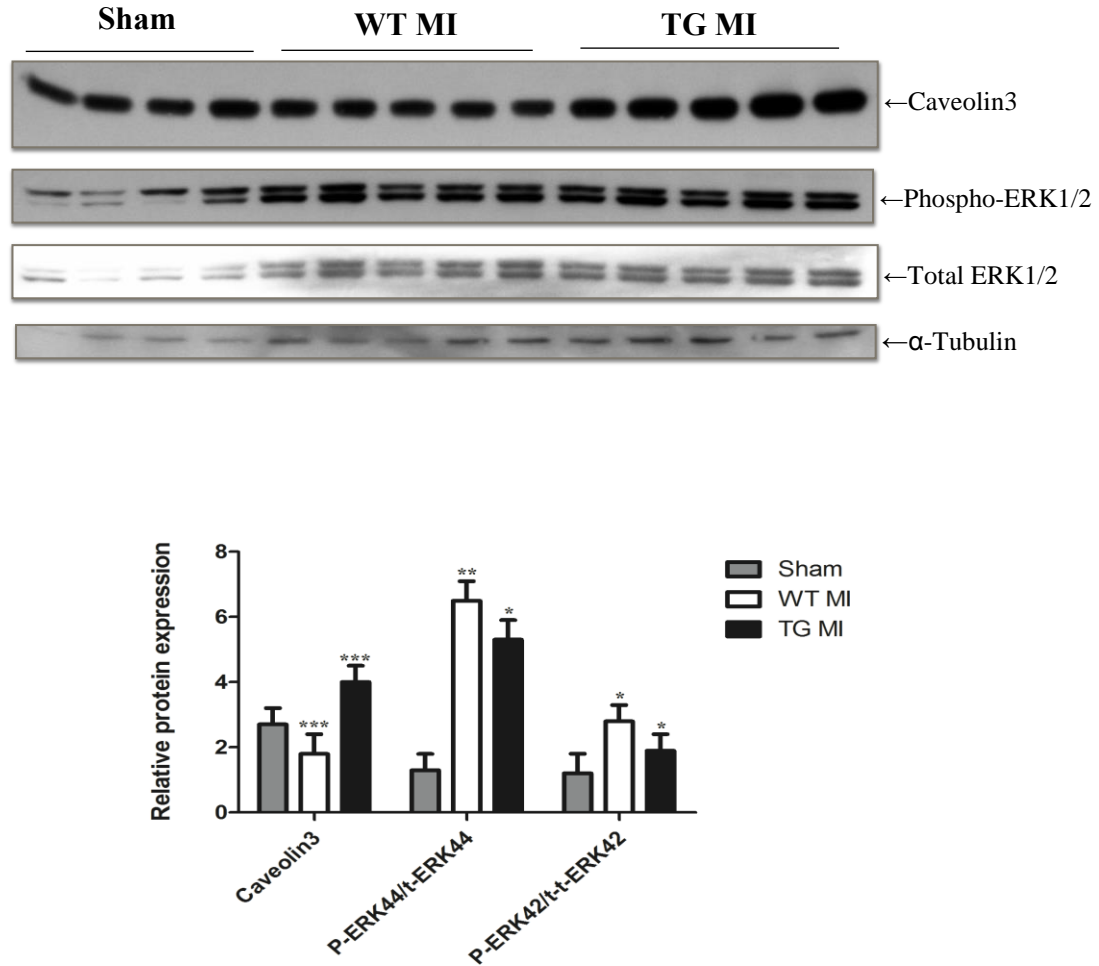
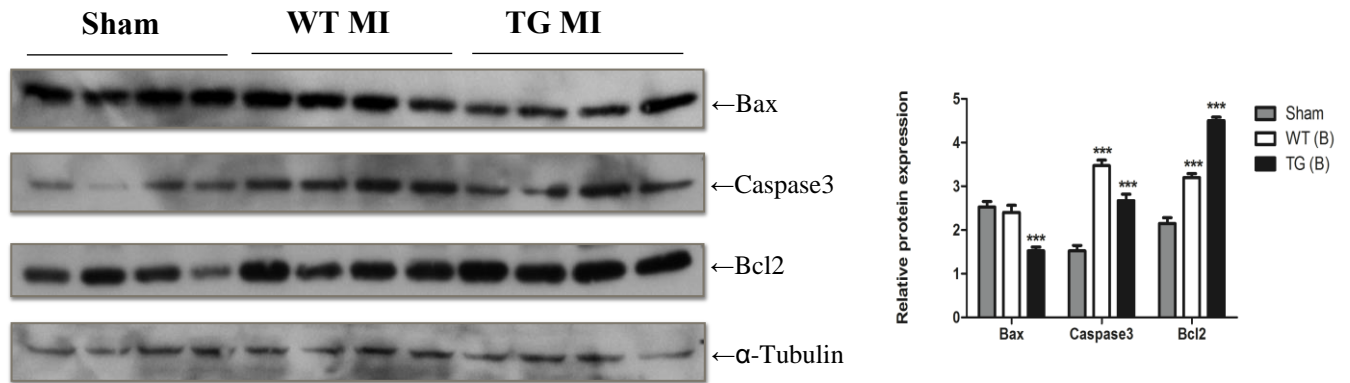


Figure 13: Expression of cardiac signaling proteins in infarct area post MI. Western blot analysis of left ventricular lysates of infarct tissue post MI shows significant upregulation of cardioprotective protein caveolin3 in SLMAP3 TG ($p < 0.001$) in comparison to WT. In contrary, the heart failure signal phosphorylated ERK1/2 were significantly higher in both MI groups ($p < 0.01$, $p < 0.05$) respectively compared to sham, but the elevation in these proteins was reduced in SLMAP3 TG ($p < 0.05$, $p < 0.05$) respectively in comparison to WT, $n = 4-5$ in each group.

Border area (B)

a.



b.

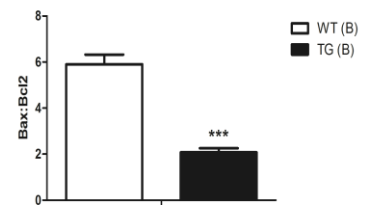


Figure 14: Expression of proapoptotic and antiapoptotic proteins in border area (B) post MI.

The same trend of data shown in infarct area was seen in the border zone of the infarct. a)

Western blot analysis of marginal tissue post MI shows elevated levels of proapoptotic proteins caspase3 as well as antiapoptotic Bcl2 in both MI's groups in comparison to sham (p<0.001, p<0.001) respectively. Surprisingly, the proapoptotic Bax & caspase3 were reduced in SLMAP3 TG MI (p<0.001, p<0.001) respectively compared to WT MI. In contrary, the antiapoptotic Bcl2 expression was significantly upregulated post MI in SLMAP3 TG (p<0.001) in comparison to WT. b) The ratio Bax:Bcl2 was measured, and shows a great reduction in apoptotic index post MI in SLMAP3 TG (p<0.001) compared to WT, n=4 in each group.

Border area (B)

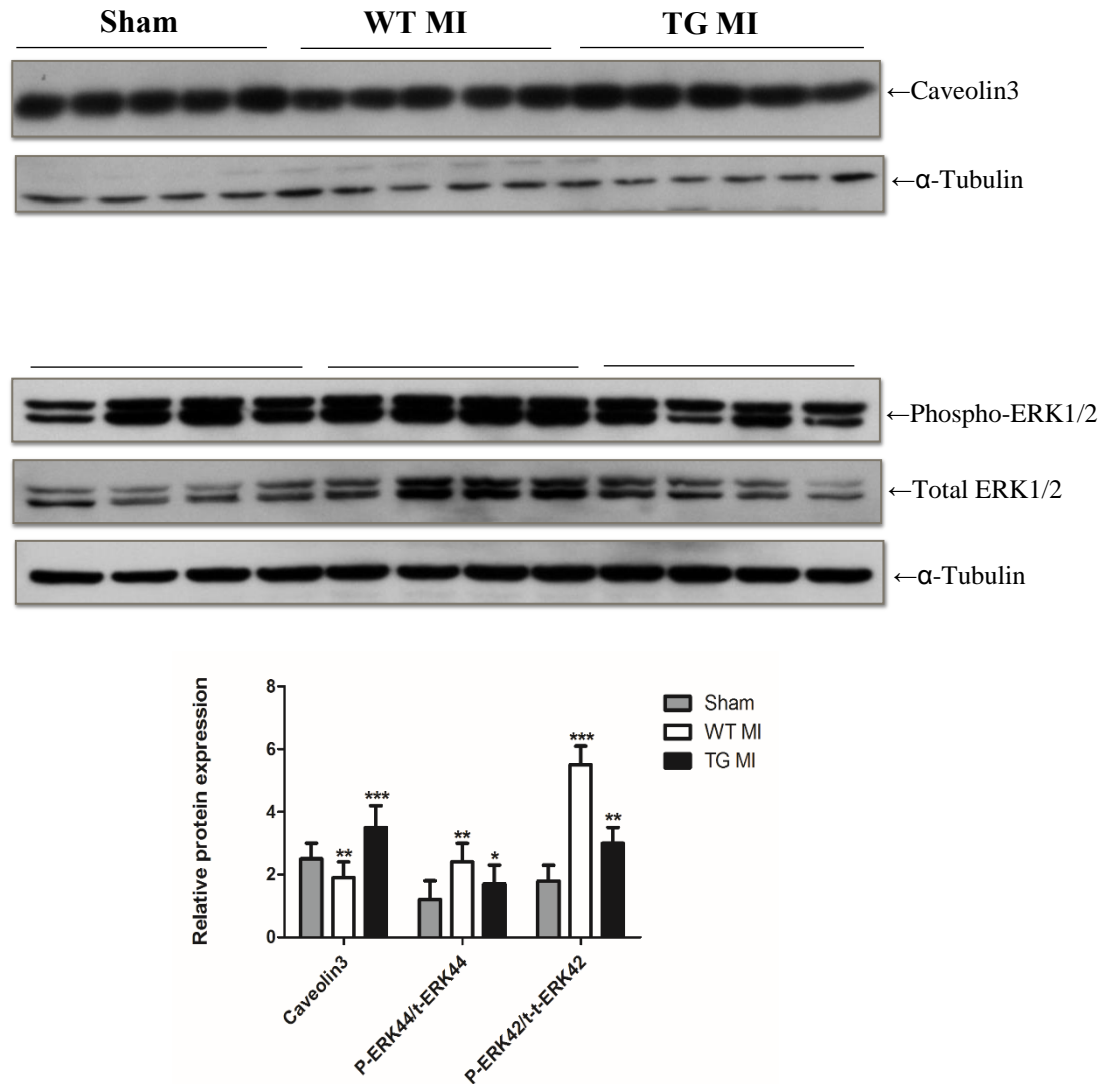
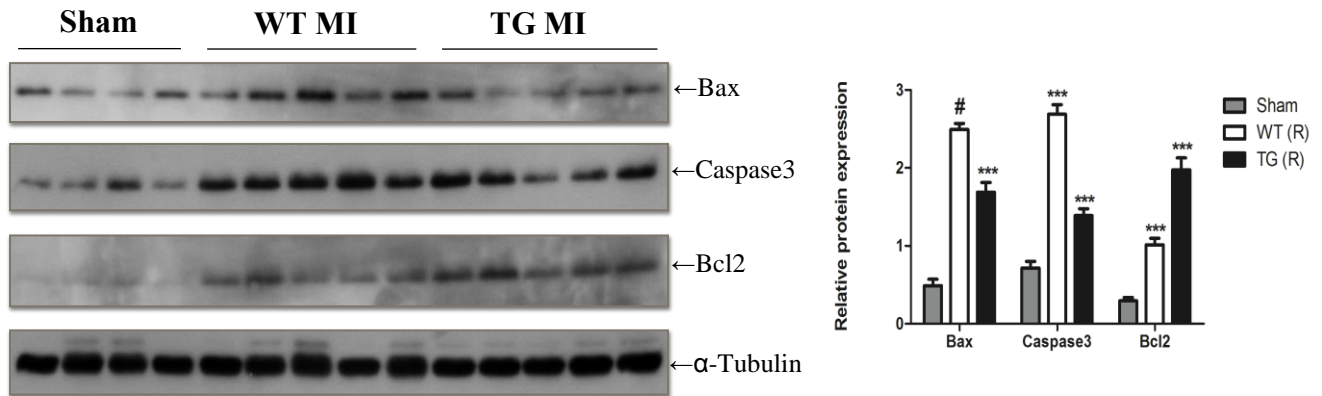


Figure 15: *Expression of cardiac signaling proteins in border area post MI.* Western blot analysis of left ventricular lysates of border tissue post MI shows significant upregulation of cardioprotective protein caveolin3 in SLMAP3 TG ($p < 0.001$) in comparison to WT. In contrary, the transcriptional factors phosphorylated ERK1/2 were significantly higher in both MI groups ($p < 0.01$, $p < 0.001$) respectively compared to sham, but the elevation in these proteins was reduced in SLMAP3 TG ($p < 0.05$, $p < 0.01$) respectively in comparison to WT, $n = 4-5$ in each group.

Remote area (R)

a.



b.

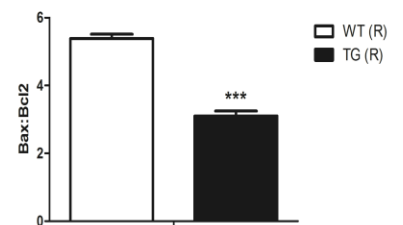


Figure 16: Expression of proapoptotic and antiapoptotic proteins in remote area (R) post MI.

The same trend of data shown in infarct and border areas post MI was seen in the remote area of the infarct. a) Western blot analysis of remote viable tissue post MI shows elevated levels of proapoptotic proteins Bax and caspase3 as well as antiapoptotic Bcl2 in both MI's groups in comparison to sham ($p < 0.001$, $p < 0.001$, $p < 0.001$) respectively. Surprisingly, the proapoptotic Bax & caspase3 were markedly reduced in SLMAP3 TG MI ($p < 0.001$, $p < 0.001$) compared to WT MI. In contrary, the antiapoptotic Bcl2 expression was significantly upregulated post MI in SLMAP3 TG ($p < 0.001$) in comparison to WT. b) The ratio Bax:Bcl2 was measured, and shows a great reduction in apoptotic index post MI in SLMAP3 TG ($p < 0.001$) compared to WT, $n = 4-5$ in each group.

Remote area (R)

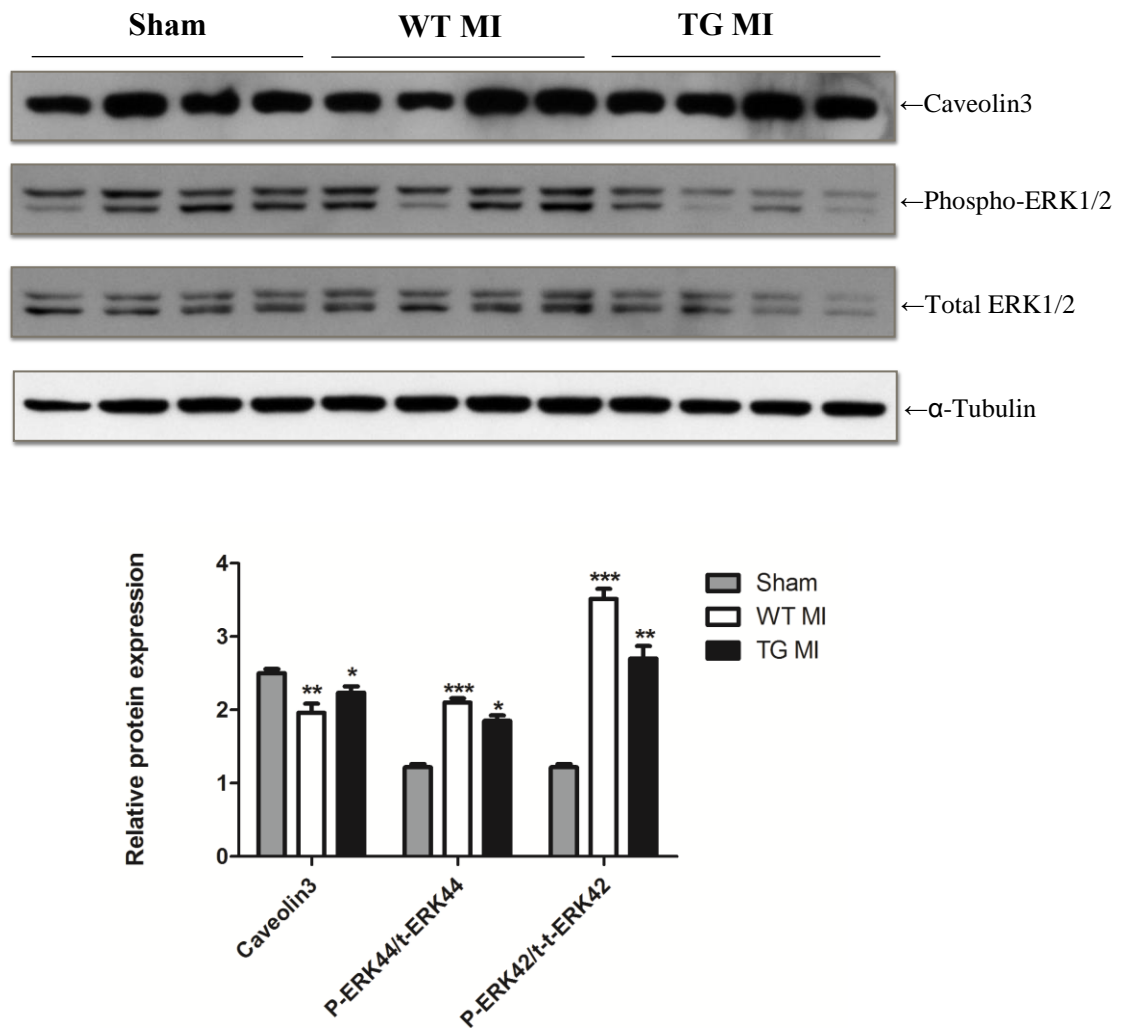


Figure 17: *Expression of cardiac signaling proteins in remote area post MI.* Western blot analysis of left ventricular lysates of remote tissue post MI shows significant upregulation of cardioprotective protein caveolin3 in SLMAP3 TG post MI ($p < 0.05$) in comparison to WT. In contrary, the transcriptional factors phosphorylated ERK1/2 were reduced in SLMAP3 TG post MI ($p < 0.05$, $p < 0.01$) respectively compared to WT MI, $n = 4$ in each group.

CHAPTER 4: DISCUSSION

Myocardial infarction and heart failure are major causes of morbidity and mortality in developed and developing countries. However, even with advanced progress in their treatment over last few years, the hopeful remedy for these diseases is still frustrating. In last few decades as well as more recently, many medications have been approved to be used in treatment and prevention of such diseases, but neither high efficiency nor low adverse effects was achieved with these medications (Reddy, 2015). For instance, fibrinolytic therapy in MI cases is associated with high major bleeding tendency and low cure rate especially if the infarct's onset passed the first few hours (Reddy, 2015). Another treatment option for MI is the coronary artery bypass graft (CABG) surgery that aims to replace the occluded coronary artery with another one to reinstate the coronary circulation has also associated with a number of life threatening complications such as the occurrence of new MI in ~7% of patients, which is called as post-CABG MI (Reddy, 2015). Taking into consideration the current hazardous and to some extent the less efficient current treatment options of MI and subsequent HF, as well as association of complicated and interactive molecular mechanisms with pathogenesis of these diseases, a new efficient and less invasive therapeutics to limit cardiac remodeling will provide a promising option in treatment of these cardiac diseases. Therefore, the cardiac research nowadays is aimed to deeply understand the different molecular mechanisms involved in cardiac remodeling and to find certain ways to manipulate such mechanisms with least possible adverse effects. For instance, cardiac stem cell therapy hugely attracted sights toward finding reparative or regenerative replacement of failing cardiomyocytes by newly differentiated ones in the cardiac remodeling diseases such that in MI and HF (Reddy, 2015). However, the success of cardiac stem cell therapy has faced some obstacles such as making these cells surviving in a dead

necrotic or an avascular fibrotic tissue, such that it occurs in myocardium in post MI (Reddy, 2015; Samuel et al., 2011). Therefore, molecular mechanisms or therapies that help to limit apoptosis as well as fibrotic tissue formation in post MI will provide de novo or adjunct therapy for treatment of cardiac remodeling in post MI.

In the current study, I emphasize the protective effects of SLMAP3 on post MI ventricular remodeling in MI mouse model. Specifically, I demonstrate that overexpressing SLMAP3 in postnatal hearts served to attenuate infarct size in the left ventricles and interstitial fibrosis (collagen density) in the whole areas of both ventricles in post MI, and this was concomitant with increased survival and partially compensated heart failure. Moreover, I found that SLMAP3 markedly reduced left ventricular dysfunction and rupture in post MI either in an acute phase or a chronic phase as well as limited apoptosis. Furthermore, SLMAP3 significantly elevated the prosurvival program in all areas of the left ventricle (Infarct, border, and remote) and simultaneously reduced the death signals in those areas. Our data here strongly suggests that SLMAP3 may function as a downstream signaling molecule that regulates post MI apoptosis, fibrosis, and membrane biology, thus enhancing the favorable left ventricular remodeling with concomitant increased survival rates in these TG mice.

I studied mice at 4 weeks post MI, representing the perfect time of mature fibrotic healing and thus the chronic left ventricular dysfunction (Rubin et al., 2005). To estimate the effects of overexpressing SLMAP3 in the heart post MI, I performed some morphometric, histological and cardiac function assessments. I found that mice with overexpressed SLMAP3 showed better cardiac pumping capacity as well as less ventricular dilation as assessed by echocardiography measurements of left ventricular wall thickness and lumen diameters in both systole and diastole (table 1, figure 4). In addition, morphometric analysis has shown that these TG mice have less

signs of developing heart failure in post MI, which was represented in a decreased lung weight to body weight ratio (table 1).

Fibrosis is still known a mechanism for infarct healing and remodeling, which prevents early myocardial rupture in post MI (Hwang et al., 2001). However, an extensive fibrotic reaction in response to inflammation and apoptosis in post MI in human hearts and in experimental MI murine model have been found to be extended to areas of remote viable myocardium as well as the right ventricle, and therefore associated with adverse left ventricular remodeling (Brower & Janicki, 2001; Bussani et al., 2003). The reactive fibrosis that is found in remote myocardium of both ventricles post MI was triggered by multiple mechanisms such as exaggerated inflammation and apoptosis, and thus the downstream molecular regulation of these pathways will limit the extensive ventricular remodeling (Erdal et al., 2012). In my study, the histological analysis of fibrosis from serial cross sections of SLMAP3 TG hearts revealed less infarct size as well as less collagen density, which was less distributed throughout all regions of the left ventricle as well as in the right ventricle (figure 7).

In myocardial infarction, necrosis and apoptosis are major pathogenesis for the development of ventricular remodeling (Olivetti et al., 1996; Wencker et al., 2003). As opposed to necrosis, apoptosis utilizes energy in a highly regulated process, which is controlled by simultaneous interactive balance of prosurvival and prodeath signals (Gill et al., 2002; Szalai et al., 1999). These signals might be activated by death receptors on cell membrane (extrinsic pathway) or by cytochrome c release from mitochondria (intrinsic or mitochondrial pathway) (Webster, 2012). In an intrinsic pathway, when mitochondria is exposed to stress such as DNA damage due to necrosis, this will lead to alterations in the mitochondrial outer membrane (MOM) permeability and subsequent release of cytochrome c into cytoplasm (Webster, 2012).

Further, cytochrome c will activate cascade of proteolytic proteins, ending up with the transformation of inactive caspase3 into active cleaved caspase3, which has unique apoptotic activity and directly mediates the DNA degradation (Webster, 2012). The mitochondrial pathway of apoptosis could be downregulated by activity of antiapoptotic Bcl2 protein, which stabilizes the MOM (Webster, 2012). On other hand, this pathway could be extremely enhanced by proapoptotic Bax protein, which increases the permeability of MOM, and thus induces cytochrome c release to cytoplasm (Webster, 2012). The net effect of these two proteins (Bcl2 and Bax) at mitochondrial level will determine the fate of cardiomyocytes either to survive or to die (Webster, 2012). Experimental murine ischemia/reperfusion study found that the Bcl2 treatment had reduced apoptosis and myocardial remodeling, and thus protected the heart (Iwata et al., 2010). Alternatively, other studies have shown that adverse cardiac remodeling post MI was associated with elevated levels of Bax and caspase3 (Webster, 2012; Whelan et al., 2012). Here in my present study, SLMAP3 served to limit apoptosis, which was assessed by TUNEL assay (figure 9) in the early 24 hours post MI, and Western blot analysis in 48 hours post MI (figure 12a, 14a, 16a). Surprisingly, overexpression of SLAMP3 served to switch the proapoptotic signals (Bax and caspase3) to antiapoptotic Bcl2 signal, which was concomitantly associated with less apoptotic index (figure 12b, 14b, 16b).

Many cardioprotective signaling pathways are found to protect the heart and enhance its performance in certain cardiac diseases such as in HF including caveolea system, which regulates antiapoptosis and suppresses the hypertrophic signals (Erdal et al., 2012; Markandeya et al., 2015). Caveolea is cave-like structures located at cell membrane and is composed of caveolins such as the ubiquitously expressed cav1 & cav2, and the muscle specific caveolin3, which is the only caveolin isoform in the heart (Horikawa et al., 2014). Alternatively, in

pathological cardiac hypertrophy, ventricular cardiomyocyte undergoes subcellular remodeling, which is associated with a reduction in the scaffolding protein cav3 concomitant with altered calcium cycling (Markandeya et al., 2015). Caveolins are involved in numerous important signal transductions inside cardiomyocytes such as calcium signaling, adrenergic signaling, and vesicular trafficking, which served as cardiac protection (Horikawa et al., 2014). Caveolins act as a scaffolding proteins via their specific scaffolding domains and serve essential roles in categorization of major signals such as MAPK, PKC, PI3K/AKT, tyrosine kinase, and ion channels of Na⁺, Ca⁺⁺, K⁺, and Cl⁻ (Horikawa et al., 2014). Many studies have found that mutations in Caveolin3 gene are associated with long QT syndrome, which leads to electrical cardiac dysfunction and sudden death (Cutler & Kaufman, 2013). Similar studies have shown that these mutations lead to defects in nitric oxide synthase (NO synthase) and alteration in the expression of sodium and potassium channels of cardiomyocytes, which therefore result in aberrant electrical activity and pathological cardiac hypertrophic remodeling (Cutler & Kaufman, 2013; Murfitt et al., 2015; Senatore et al., 2014). In similar way, SLMAP3 has been found to be involved in Na⁺ channel trafficking, and two missense mutations in SLMAP3 gene found to be linked with channelopathy disorder known as Brugada syndrome, which leads to impaired electrical cardiac activity and death (Ishikawa et al., 2012). Overexpression of Cav3 is found to be protective against pathological cardiac hypertrophy via PKC-Calcium mechanism, NO synthase signaling, and restoration of adrenergic receptors to T-tubules through cAMP signaling in these studies (Cutler & Kaufman, 2013; Horikawa et al., 2014; Wright et al., 2014) respectively. On the other hand cav3 knockout in mice has shown adverse cardiac dysfunction via activation of ERK1/2 signaling pathway (Woodman et al., 2002). In the same study, cav3 knockout mice showed a range of cardiac pathologies such as cardiac hypertrophy and dilated

cardiomyopathy concomitant with reduced fractional shortening as assessed by echocardiography (Woodman et al., 2002). Furthermore, Ras-ERK1/2 signal was activated in these mice, which was assessed by elevated levels of phosphorylated ERK1/2 (Woodman et al., 2002). Taking all together the protective roles of caveolin3 and its negative regulation of the well-known mechanism ERK1/2 in pathological cardiac hypertrophy, the mechanisms that elevate caveolin3 and downregulate phosphorylated ERK1/2 in the heart eventually will be protective. In the present study, throughout all regions of the left ventricle post MI, SLMAP3 significantly upregulated caveolin3 as well as markedly downregulated the levels of phosphorylated ERK1/2 (figure 13, 15, 17); suggesting protective mechanisms were triggered by SLMAP3. In addition, considering the involvement of SLMAP3 in normal membrane biology, and the regulation of excitation contraction coupling inside cardiomyocytes as well as facilitation of sodium channel trafficking on cardiomyocyte surface, these mechanisms are very critical in ventricular remodeling and if maintained in post MI, functionality of cardiomyocytes will be to some extent restored (Duarte-Costa et al., 2014; Erdal et al., 2012; Markandeya et al., 2015). In my study, endogenous levels of SLMAP3 in infarct as well as remote myocardium of the left ventricle were significantly elevated post MI (figure 11), suggesting that the protective effects were triggered and mediated by this protein.

Heart failure is the hallmark adverse effect of MI. Thus, molecular study of HF biomarkers would help to support my study. Galectin3 is one of the recent HF biomarkers that is, in addition to being a helpful tool for detection of HF development in post MI, it is also a prognostic factor for this disease, whereas the highest galectin3 level in the heart is the severely developed HF (Leone & Iacoviello, 2015; Sharma et al., 2004). Human galectin3 gene found to play important role in cell growth, differentiation and cancer (Duneau et al., 2005). Alternatively,

this gene encodes protein that has been involved in the intracellular mitochondrial apoptotic activity via enhancing release of cytochrome c from mitochondria concomitant with suppression of antiapoptotic Bcl-xL (Duneau et al., 2005). Later study has found that galectin3 gene encoded mitogaligin protein, which was sublocalized to mitochondrial membranes and nuclei through two specific sequences, and induced the intracellular cytotoxic effect and apoptosis (Gonzalez et al., 2009). Taking into account, the implication of galectin3 in heart failure and myocardial remodeling as well as triggering of intracellular apoptosis, galectin3 levels were assessed in my project by Western blot as well as immunohistochemistry. Surprisingly, galectin3 expression in infarct as well as border area was markedly reduced by SLMAP3 overexpression post MI (figure 6A, B).

Whether such potential roles make SLMAP3 overexpressed mice survive longer post MI or not are difficult to suggest. Therefore, mice were monitored over one year for death records and the reason of the death was explored. Interestingly, no deaths were recorded in SLMAP3 overexpressed mice, while as 70% of WT mice died (figure 5). Furthermore, mice which survived after one year were sacrificed and examined in order to check the morphology and the histology, and discern why these SLMAP3 TG mice survived. Most of SLMAP3 hearts showed symmetrical global appearance with almost no demarcation lines of infarct among the left ventricles. Furthermore, these hearts were notably red (more vascular), which may suggest the growth of new blood vessels (figure 8A, B). On the contrary, the remaining WT hearts which survived after MI showed asymmetrical balloon like dilation at infarct area, which was delicate and appeared as a well-demarcated area among the left ventricle. In addition, this dilation was notably pale (less vascular), suggesting impending rupture in these hearts. Furthermore, histological appearance of Masson's trichrome (MT) and hematoxylin and Eosin (H&E) stained

myocardium showed likely enhanced growth of new muscular tissues and blood vessels at the site of infarct in SLMAP3 myocardium in comparison to WT, which may suggest another possible protective mechanism that might be triggered by SLMAP3 (figure 8A, B). However, further work in the future should be done on SLMAP3 aiming to quantify the blood vessels and myocyte's number and size at infarct and adjacent myocardium, and furthermore to explore the possible molecular mechanisms by which SLMAP3 might enhance blood vessel formation as well as muscle growth.

CONCLUSION

In view of my findings in the current study, SLMAP3 served to attenuate the left ventricular remodeling in post MI in MI mouse model. Overexpression of SLMAP3 in postnatal heart preserved cardiac performance concomitantly with less left ventricular dilation post MI. In addition, SLMAP3 TG mice showed signs of compensating the heart failure as well as an increase in the longevity of mice post MI. Furthermore, apoptosis and interstitial fibrosis post MI in infarct as well as in remote viable myocardium were diminished by SLMAP3. Cardioprotective mechanisms as well as prosurvival signals were enhanced by SLMAP3, while concomitantly the prodeath signals were markedly reduced.

In previously published work in our lab, SLAMPs played a distinct role in membrane biology, cell growth, and regulation of excitation-contraction apparatus in cardiomyocytes. Thus, here we propose that strategies to induce SLMAP3 levels in heart may represent a potential new therapeutic target in the treatment and preservation of myocardium post MI and HF.

CHAPTER FIVE: REFERENCES

- Ahmed, N., Dawson, M., Smith, C., & Wood, E. (2007). *Biology of Disease*.
- Alcalay, Y., Hochhauser, E., Kliminski, V., Dick, J., Zahalka, M. A., Parnes, D., ... Kessler-Icekson, G. (2013). Popeye Domain Containing 1 (Popdc1/Bves) Is a Caveolae-Associated Protein Involved in Ischemia Tolerance. *PLoS ONE*, 8(9).
<http://doi.org/10.1371/journal.pone.0071100>
- Ali, I. U., Lidereau, R., & Callahan, R. (1989). Presence of two members of c-erbA receptor gene family (c-erbA beta and c-erbA2) in smallest region of somatic homozygosity on chromosome 3p21-p25 in human breast carcinoma. *Journal of the National Cancer Institute*, 81(23), 1815–1820.
- Amarante-Mendes, G. P., Naekyung Kim, C., Liu, L., Huang, Y., Perkins, C. L., Green, D. R., & Bhalla, K. (1998). Bcr-Abl exerts its antiapoptotic effect against diverse apoptotic stimuli through blockage of mitochondrial release of cytochrome C and activation of caspase-3. *Blood*, 91(5), 1700–5. Retrieved from <http://www.ncbi.nlm.nih.gov/pubmed/9473236>
- Antzelevitch, C., & Patocskai, B. (2016). Brugada Syndrome: Clinical, Genetic, Molecular, Cellular, and Ionic Aspects. *Current Problems in Cardiology*, 41(1), 7–57.
<http://doi.org/10.1016/j.cpcardiol.2015.06.002>
- Barman, S. a, Zhu, S., Han, G., & White, R. E. (2003). cAMP activates BKCa channels in pulmonary arterial smooth muscle via cGMP-dependent protein kinase. *American Journal of Physiology. Lung Cellular and Molecular Physiology*, 284(6), L1004–L1011.
<http://doi.org/10.1152/ajplung.00295.2002>

- Belge, C., Hammond, J., Dubois-Deruy, E., Manoury, B., Hamelet, J., Beauloye, C., ...
Balligand, J. L. (2014). Enhanced expression of β 3-adrenoceptors in cardiac myocytes attenuates neurohormone-induced hypertrophic remodeling through nitric oxide synthase. *Circulation*, 129(4), 451–462. <http://doi.org/10.1161/CIRCULATIONAHA.113.004940>
- Brand, N. J., & Barton, P. J. R. (2002). Myocardial molecular biology: an introduction. *Heart (British Cardiac Society)*, 87(3), 284–93. <http://doi.org/10.1136/heart.87.3.284>
- Brower, G. L., & Janicki, J. S. (2001). Contribution of ventricular remodeling to pathogenesis of heart failure in rats. *Am.J.Physiol Heart Circ.Physiol*, 280(2), H674–H683.
- Bueno, O. F., De Windt, L. J., Tymitz, K. M., Witt, S. A., Kimball, T. R., Klevitsky, R., ...
Molkentin, J. D. (2000). The MEK1-ERK1/2 signaling pathway promotes compensated cardiac hypertrophy in transgenic mice. *The EMBO Journal*, 19(23), 6341–50.
<http://doi.org/10.1093/emboj/19.23.6341>
- Burack, W. R., & Shaw, A. S. (2000). Signal transduction: Hanging on a scaffold. *Current Opinion in Cell Biology*. [http://doi.org/10.1016/S0955-0674\(99\)00078-2](http://doi.org/10.1016/S0955-0674(99)00078-2)
- Bussani, R., Abbate, a, Biondi-Zoccai, G. G. L., Dobrina, a, Leone, a M., Camilot, D., ...
Baldi, a. (2003). Right ventricular dilatation after left ventricular acute myocardial infarction is predictive of extremely high peri-infarctual apoptosis at postmortem examination in humans. *Journal of Clinical Pathology*, 56(9), 672–676.
<http://doi.org/10.1136/jcp.56.9.672>
- Byers, J. T., Guzzo, R. M., Salih, M., & Tuana, B. S. (2009). Hydrophobic profiles of the tail anchors in SLMAP dictate subcellular targeting. *BMC Cell Biology*, 10, 48.

<http://doi.org/10.1186/1471-2121-10-48>

Cabrera-Vera, T. M., Vanhauwe, J., Thomas, T. O., Medkova, M., Preininger, A., Mazzoni, M.

R., & Hamm, H. E. (2003). Insights into G Protein Structure, Function, and Regulation.

Endocrine Reviews. <http://doi.org/10.1210/er.2000-0026>

Chatzifrangkeskou, M., Dour, C. Le, Wu, W., Morrow, J. P., Joseph, L. C., Beuvin, M., ...

Muchir, A. (2016). ERK1/2 directly acts on CTGF/CCN2 expression to mediate myocardial fibrosis in cardiomyopathy caused by mutations in the lamin A/C gene. *Human Molecular Genetics*, 25(8), 1–14.

<http://doi.org/10.1093/hmg/ddw090>

Chen, X., & Ding, H. (2011). Increased expression of the tail-anchored membrane protein

SLMAP in adipose tissue from type 2 tally ho diabetic mice. *Experimental Diabetes Research*, 2011.

<http://doi.org/10.1155/2011/421982>

Cheng, W., Kajstura, J., Nitahara, J. A., Li, B., Reiss, K., Liu, Y., ... Anversa, P. (1996).

Programmed myocyte cell death affects the viable myocardium after infarction in rats.

Experimental Cell Research, 226(2), 316–327. <http://doi.org/10.1006/excr.1996.0232>

Chuang, S. M., Wang, I. C., & Yang, J. L. (2000). Roles of JNK, p38 and ERK mitogen-

activated protein kinases in the growth inhibition and apoptosis induced by cadmium.

Carcinogenesis, 21(7), 1423–1432. Retrieved from

http://www.ncbi.nlm.nih.gov/entrez/query.fcgi?cmd=Retrieve&db=PubMed&dopt=Citation&list_uids=10874022

Cohen, P. (2002). The origins of protein phosphorylation. *Nature Cell Biology*, 4(5), E127–

E130. <http://doi.org/10.1038/ncb0502-e127>

- Cohn, J. N., Ferrari, R., & Sharpe, N. (2000). Cardiac remodeling-concepts and clinical implications: A consensus paper from an International Forum on Cardiac Remodeling. *Journal of the American College of Cardiology*, 35(3), 569–582.
[http://doi.org/10.1016/S0735-1097\(99\)00630-0](http://doi.org/10.1016/S0735-1097(99)00630-0)
- Cotran, R. S., & Robbins, S. L. (1997). *Basic Pathology Sixth Edition*. W. B. Saunders Company.
- Crocker, J., & Murray, P. G. (2003). *Molecular Biology in Cellular Pathology. Molecular Biology* (Vol. 20). <http://doi.org/10.1111/j.1471-4159.2011.07232.x>
- Crompton, M. (1999). The mitochondrial permeability transition pore and its role in cell death. *The Biochemical Journal*, 341 (Pt 2, 233–249. <http://doi.org/10.1007/s10495-007-0723-y>
- Crone, S. a, Zhao, Y.-Y., Fan, L., Gu, Y., Minamisawa, S., Liu, Y., ... Lee, K.-F. (2002). ErbB2 is essential in the prevention of dilated cardiomyopathy. *Nature Medicine*, 8(5), 459–465.
<http://doi.org/10.1038/nm0502-459>
- Cutler, M. J., & Kaufman, E. S. (2013). To be or not to be: Long-QT syndrome type 9. *Circulation: Cardiovascular Genetics*, 6(5), 439–440.
<http://doi.org/10.1161/CIRCGENETICS.113.000345>
- Desagher, S., & Martinou, J. C. (2000). Mitochondria as the central control point of apoptosis. *Trends in Cell Biology*. [http://doi.org/10.1016/S0962-8924\(00\)01803-1](http://doi.org/10.1016/S0962-8924(00)01803-1)
- Ding, H., Howarth, A. G., Pannirselvam, M., Anderson, T. J., Severson, D. L., Wiehler, W. B., ... Tuana, B. S. (2005). Endothelial dysfunction in Type 2 diabetes correlates with deregulated expression of the tail-anchored membrane protein SLMAP. *American Journal of Physiology. Heart and Circulatory Physiology*, 289(1), H206–11.

<http://doi.org/10.1152/ajpheart.00037.2005>

Duarte-Costa, S., Castro-Ferreira, R., Neves, J. S., & Leite-Moreira, A. F. (2014). S100A1: A major player in cardiovascular performance. *Physiological Research*.

Duneau, M., Boyer-Guittaut, M., Gonzalez, P., Charpentier, S., Normand, T., Dubois, M., ... Legrand, A. (2005). Galig, a novel cell death gene that encodes a mitochondrial protein promoting cytochrome c release. *Experimental Cell Research*, 302(2), 194–205.

<http://doi.org/10.1016/j.yexcr.2004.08.041>

Dzimiri, N. (2002). Receptor crosstalk. Implications for cardiovascular function, disease and therapy. *European Journal of Biochemistry*, 269(19), 4713–4730. <http://doi.org/3181> [pii]

Eapen, Z. J., Tang, W. H. W., Felker, G. M., Hernandez, A. F., Mahaffey, K. W., Lincoff, A. M., & Roe, M. T. (2012). Defining heart failure end points in ST-segment elevation myocardial infarction trials: Integrating past experiences to chart a path forward. *Circulation: Cardiovascular Quality and Outcomes*, 5(4), 594–600.

<http://doi.org/10.1161/CIRCOUTCOMES.112.966150>

English, J. M., & Cobb, M. H. (2002). Pharmacological inhibitors of MAPK pathways. *Trends in Pharmacological Sciences*. [http://doi.org/10.1016/S0165-6147\(00\)01865-4](http://doi.org/10.1016/S0165-6147(00)01865-4)

Erdal, C., Karakulah, G., Fermancı, E., Kunter, I., Silistreli, E., Canda, T., ... Hepaguslar, H. (2012). Early biventricular molecular responses to an acute myocardial infarction. *International Journal of Medical Sciences*, 9(1), 74–82. <http://doi.org/10.7150/ijms.9.74>

Finucane, D. M., Bossy-Wetzell, E., Waterhouse, N. J., Cotter, T. G., & Green, D. R. (1999). Bax-induced caspase activation and apoptosis via cytochrome c release from mitochondria

is inhibitable by Bcl-xL. *Journal of Biological Chemistry*, 274(4), 2225–2233.

<http://doi.org/10.1074/jbc.274.4.2225>

Frangogiannis, N. G. (2008). The immune system and cardiac repair. *Pharmacological Research*, 58(2), 88–111. <http://doi.org/10.1016/j.phrs.2008.06.007>

Gill, C., Mestril, R., & Samali, A. (2002). Losing heart: the role of apoptosis in heart disease--a novel therapeutic target. *The FASEB Journal : Official Publication of the Federation of American Societies for Experimental Biology*, 16, 135–146. <http://doi.org/10.1096/fj.01-0629com>

Gonzalez, P., Robinet, P., Charpentier, S., Mollet, L., Normand, T., Dubois, M., & Legrand, A. (2009). Apoptotic activity of a nuclear form of mitogaligin, a cell death protein. *Biochemical and Biophysical Research Communications*, 378(4), 816–820. <http://doi.org/10.1016/j.bbrc.2008.11.133>

Guzzo, R. M., Salih, M., Moore, E. D., & Tuana, B. S. (2005). Molecular properties of cardiac tail-anchored membrane protein SLMAP are consistent with structural role in arrangement of excitation-contraction coupling apparatus. *American Journal of Physiology. Heart and Circulatory Physiology*, 288(4), H1810–9. <http://doi.org/10.1152/ajpheart.01015.2004>

Guzzo, R. M., Sevinc, S., Salih, M., & Tuana, B. S. (2004). A novel isoform of sarcolemmal membrane-associated protein (SLMAP) is a component of the microtubule organizing centre. *Journal of Cell Science*, 117(Pt 11), 2271–81. <http://doi.org/10.1242/jcs.01079>

Guzzo, R. M., Wigle, J., Salih, M., Moore, E. D., & Tuana, B. S. (2004). Regulated expression and temporal induction of the tail-anchored sarcolemmal-membrane-associated protein is

critical for myoblast fusion. *The Biochemical Journal*, 381(Pt 3), 599–608.

<http://doi.org/10.1042/BJ20031723>

Hahn, H. S., Marreez, Y., Odley, A., Sterbling, A., Yussman, M. G., Hilty, K. C., ... Dorn, G. W. (2003). Protein kinase Calpha negatively regulates systolic and diastolic function in pathological hypertrophy. *Circ Res*, 93, 1111–1119.

<http://doi.org/10.1161/01.RES.0000105087.79373.17>

Hausdorff, W. P., Caron, M. G., & Lefkowitz, R. J. (1990). Turning off the signal:

desensitization of beta-adrenergic receptor function. *The FASEB Journal*, 4(11), 2881–2889. Retrieved from

<http://www.fasebj.org/content/4/11/2881>\n<http://www.fasebj.org/content/4/11/2881.full.pdf>\n<http://www.fasebj.org/content/4/11/2881.short>\n<http://www.ncbi.nlm.nih.gov/pubmed/2165947>

He, Y.-Y., Liu, C.-L., Li, X., Zhong, W., Li, S., He, K.-L., & Wang, L.-L. (2014). Effects of PP1-12, a Novel Protein Phosphatase-1 Inhibitor, on Ventricular Function and Remodeling After Myocardial Infarction in Rats. *Journal of Cardiovascular Pharmacology*, 64(4), 360–7. <http://doi.org/10.1097/FJC.0000000000000128>

Hernandez-Resendiz, S., & Zazueta, C. (2014). PHO-ERK1/2 interaction with mitochondria regulates the permeability transition pore in cardioprotective signaling. *Life Sciences*, 108(1), 13–21. <http://doi.org/10.1016/j.lfs.2014.04.037>

Horikawa, Y. T., Tsutsumi, Y. M., Patel, H. H., & Roth, D. M. (2014). Signaling epicenters: The role of caveolae and caveolins in volatile anesthetic induced cardiac protection. *Current Pharmaceutical Design*, 20(36), 5681–5689. Retrieved from

<http://www.scopus.com/inward/record.url?eid=2-s2.0-84925781297&partnerID=tZOtx3y1>

- Hwang, M. W., Matsumori, A., Furukawa, Y., Ono, K., Okada, M., Iwasaki, A., ... Sasayama, S. (2001). Neutralization of interleukin-1 β in the acute phase of myocardial infarction promotes the progression of left ventricular remodeling. *Journal of the American College of Cardiology*, 38(5), 1546–1553. [http://doi.org/10.1016/S0735-1097\(01\)01591-1](http://doi.org/10.1016/S0735-1097(01)01591-1)
- Iryo, Y., Matsuoka, M., & Wispriyono, B. (2000). Involvement of the Extracellular Signal-Regulated Protein Kinase (ERK) Pathway in the Induction of Apoptosis by Cadmium Chloride in CCRF-CEM Cells, 60(00), 1875–1882.
- Ishikawa, T., Sato, A., Marcou, C. A., Tester, D. J., Ackerman, M. J., Crotti, L., ... Kimura, A. (2012). A novel disease gene for Brugada syndrome: Sarcolemmal membrane-associated protein gene mutations impair intracellular trafficking of hNav1.5. *Circulation: Arrhythmia and Electrophysiology*, 5(6), 1098–1107. <http://doi.org/10.1161/CIRCEP.111.969972>
- Iwata, A., Morgan-Stevenson, V., Schwartz, B., Liu, L., Tupper, J., Zhu, X., ... Winn, R. (2010). Extracellular BCL2 proteins are danger-associated molecular patterns that reduce tissue damage in murine models of ischemia-reperfusion injury. *PLoS ONE*, 5(2). <http://doi.org/10.1371/journal.pone.0009103>
- Kehat, I., & Molkenin, J. D. (2010). Molecular pathways underlying cardiac remodeling during pathophysiological stimulation. *Circulation*, 122(25), 2727–2735. <http://doi.org/10.1161/CIRCULATIONAHA.110.942268>
- Kong, P., Christia, P., & Frangogiannis, N. G. (2014). The pathogenesis of cardiac fibrosis. *Cellular and Molecular Life Sciences*. <http://doi.org/10.1007/s00018-013-1349-6>

- Krupnick, J. G., & Benovic, J. L. (1998). The role of receptor kinases and arrestins in G protein-coupled receptor regulation. *Annu Rev Pharmacol Toxicol*, 38, 289–319.
<http://doi.org/10.1146/annurev.pharmtox.38.1.289>
- Kumar, P., & Clark, M. L. (2009). *Kumar and Clark's Clinical Medicine, 7th Edition*. ELSEVIER SAUNDERS. <http://doi.org/10.1016/B978-0-7020-2993-6.00027-4>
- Lemery, R., Brugada, P., Della Bella, P., Dugernier, T., van den Dool, A., & Wellens, H. J. (1989). Nonischemic Ventricular Tachycardia: Clinical Course and Long-term Follow-up in Patients Without Clinically Overt Heart Disease. *Circulation*, 79, 990–999.
<http://doi.org/10.1161/01.CIR.79.5.990>
- Leone, M., & Iacoviello, M. (2015). The predictive value of plasma biomarkers in discharged heart failure patients: role of galectin-3. *Minerva Cardioangiologica*. Retrieved from <http://www.ncbi.nlm.nih.gov/pubmed/26426300>
- Li, P., Nijhawan, D., Budihardjo, I., Srinivasula, S. M., Ahmad, M., Alnemri, E. S., & Wang, X. (1997). Cytochrome c and dATP-dependent formation of Apaf-1/caspase-9 complex initiates an apoptotic protease cascade. *Cell*, 91(4), 479–89. [http://doi.org/10.1016/S0092-8674\(00\)80434-1](http://doi.org/10.1016/S0092-8674(00)80434-1)
- Li, S., Morley, M., Lu, M., Zhou, S., Stewart, K., French, C. A., ... Morrisey, E. E. (2016). Foxp transcription factors suppress a non-pulmonary gene expression program to permit proper lung development. *Developmental Biology*, 416(2), 338–346.
<http://doi.org/10.1016/j.ydbio.2016.06.020>
- Lincoln, T. M., Dey, N., & Sellak, H. (2001). cGMP-dependent protein kinase signaling

- mechanisms in smooth muscle: from the regulation of tone to gene expression. *J. Appl. Physiol.*, 91(3), 1421–1430. <http://doi.org/10.1152/jappphysiol.00017.2004>
- Lu, S., Du, P., Shan, C., Wang, Y., Ma, C., & Dong, J. (2016). AC. *Biochemical and Biophysical Research Communications*. <http://doi.org/10.1016/j.bbrc.2016.09.012>
- Ma, L.-N., Li, L., Li, S.-C., Hao, X.-M., Zhang, J.-Y., He, P., & Li, Y.-K. (2016). Allicin improves the cardiac function by protecting against apoptosis in rat model of myocardial infarction. *Chinese Journal of Integrative Medicine*, (100029), 1–9. <http://doi.org/10.1007/s11655-016-2523-0>
- Makarewich, C. A., Zhang, H., Davis, J., Correll, R. N., Trappanese, D. M., Hoffman, N. E., ... Houser, S. R. (2014). Transient receptor potential channels contribute to pathological structural and functional remodeling after myocardial infarction. *Circulation Research*, 115(6), 567–580. <http://doi.org/10.1161/CIRCRESAHA.115.303831>
- Malo, E., Postnikoff, S. D. L., Arnason, T. G., & Harkness, T. A. A. (2016). Mitotic degradation of yeast Fkh1 by the Anaphase Promoting Complex is required for normal longevity , genomic stability and stress resistance, 8(4), 1–21.
- Manning, G., Whyte, D. B., Martinez, R., Hunter, T., Sudarsanam, S., Hunter, T., ... Bork, P. (2002). The protein kinase complement of the human genome. *Science (New York, N.Y.)*, 298(5600), 1912–34. <http://doi.org/10.1126/science.1075762>
- Marín-García, J. (2016). Cell death in the pathogenesis and progression of heart failure. *Heart Failure Reviews*, 21(2), 117–121. <http://doi.org/10.1007/s10741-016-9538-7>
- Markandeya, Y. S., Phelan, L. J., Woon, M. T., Keefe, A. M., Reynolds, C. R., August, B. K., ...

- Balijepalli, R. C. (2015). Caveolin-3 overexpression attenuates cardiac hypertrophy via inhibition of T-type Ca^{2+} current modulated by protein kinase C?? in cardiomyocytes. *Journal of Biological Chemistry*, 290(36), 22085–22100.
<http://doi.org/10.1074/jbc.M115.674945>
- Mattiazzi, A., Bassani, R. A., Escobar, A. L., Palomeque, J., Valverde, C. A., Vila Petroff, M., & Bers, D. M. (2015). Chasing cardiac physiology and pathology down the CaMKII cascade. *American Journal of Physiology. Heart and Circulatory Physiology*, 308(10), H1177–91.
<http://doi.org/10.1152/ajpheart.00007.2015>
- McCance, Kathryn L. Huether, Sue E. Brashers, Valentina. Rote, N. S. (2010). *Pathophysiology The Biologic Basic Disease in Adults and Children. Mosby ELSEVER* (Vol. 53).
<http://doi.org/10.1017/CBO9781107415324.004>
- Mehrhof, F. B., Müller, F., Bergmann, M. W., Li, P., Wang, Y., Schmitz, W., ... Harsdorf, R. Von. (2001). Activation of the Transcription Factor cAMP Response Element – Binding Protein. *American Heart Association*, 104, 2088–2095.
- Mezzaroma, E., Toldo, S., Farkas, D., Seropian, I. M., Van Tassell, B. W., Salloum, F. N., ... Abbate, A. (2011). The inflammasome promotes adverse cardiac remodeling following acute myocardial infarction in the mouse. *Proceedings of the National Academy of Sciences of the United States of America*, 108(49), 19725–30.
<http://doi.org/10.1073/pnas.1108586108>
- Molenaar, P., Chen, L., Semmler, a B. T., Parsonage, W. a, & Kaumann, a J. (2007). Human heart beta-adrenoceptors: beta1-adrenoceptor diversification through “affinity states” and polymorphism. *Clinical and Experimental Pharmacology & Physiology*, 34(December

2006), 1020–1028. <http://doi.org/10.1111/j.1440-1681.2007.04730.x>

Murfitt, L., Whiteley, G., Iqbal, M. M., & Kitmitto, A. (2015). Targeting caveolin-3 for the treatment of diabetic cardiomyopathy. *Pharmacology and Therapeutics*, *151*, 50–71. <http://doi.org/10.1016/j.pharmthera.2015.03.002>

Nader, M., Westendorp, B., Hawari, O., Salih, M., Stewart, A. F. R., Leenen, F. H. H., & Tuana, B. S. (2012). Tail-anchored membrane protein SLMAP is a novel regulator of cardiac function at the sarcoplasmic reticulum. *American Journal of Physiology. Heart and Circulatory Physiology*, *302*(5), H1138–45. <http://doi.org/10.1152/ajpheart.00872.2011>

Neet, K., & Hunter, T. (1996). Vertebrate non-receptor protein-tyrosine kinase families. *Genes to Cells : Devoted to Molecular & Cellular Mechanisms*, *1*(2), 147–69. Retrieved from <http://www.ncbi.nlm.nih.gov/pubmed/9140060>

Olivetti, G., Quaini, F., Sala, R., Lagrasta, C., Corradi, D., Bonacina, E., ... Anversa, P. (1996). Acute myocardial infarction in humans is associated with activation of programmed myocyte cell death in the surviving portion of the heart. *Journal of Molecular and Cellular Cardiology*, *28*(9), 2005–16. <http://doi.org/10.1006/jmcc.1996.0193>

Penna, C., Mancardi, D., Raimondo, S., Geuna, S., & Pagliaro, P. (2008). The paradigm of postconditioning to protect the heart: Molecular Medicine. *Journal of Cellular and Molecular Medicine*, *12*(2), 435–458. <http://doi.org/10.1111/j.1582-4934.2007.00210.x>

Pfeffer, J. M., Pfeffer, M. a, & Braunwald, E. (1985). Influence of chronic captopril therapy on the infarcted left ventricle of the rat. *Circulation Research*, *57*, 84–95. <http://doi.org/10.1161/01.RES.57.1.84>

- Pike, B. L., Hammet, A., & Heierhorst, J. (2001). Role of the N-terminal Forkhead-associated Domain in the Cell Cycle Checkpoint Function of the Rad53 Kinase. *Journal of Biological Chemistry*, 276(17), 14019–14026. <http://doi.org/10.1074/jbc.M009558200>
- Reddy, K. (2015). Recent advances in the diagnosis and treatment of acute myocardial infarction. *World Journal of Cardiology*, 7(5), 243. <http://doi.org/10.4330/wjc.v7.i5.243>
- Rosse, C., Linch, M., Kermorgant, S., Cameron, A. J. M., Boeckeler, K., & Parker, P. J. (2010). PKC and the control of localized signal dynamics. *Nature Reviews. Molecular Cell Biology*, 11(2), 103–112. <http://doi.org/10.1038/nrm2847>
- Rossé, T., Olivier, R., Monney, L., Rager, M., Conus, S., Fellay, I., ... Borner, C. (1998). Bcl-2 prolongs cell survival after Bax-induced release of cytochrome c. *Nature*, 391(6666), 496–499. <http://doi.org/10.1038/35160>
- Ruehr, M. L., Russell, M. A., & Bond, M. (2004). A-kinase anchoring protein targeting of protein kinase A in the heart. *Journal of Molecular and Cellular Cardiology*. <http://doi.org/10.1016/j.yjmcc.2004.04.017>
- Samuel, C. S., Cendrawan, S., Gao, X.-M., Ming, Z., Zhao, C., Kiriazis, H., ... Du, X.-J. (2011). Relaxin remodels fibrotic healing following myocardial infarction. *Laboratory Investigation; a Journal of Technical Methods and Pathology*, 91(5), 675–690. <http://doi.org/10.1038/labinvest.2010.198>
- Samuel, C. S., Du, X. J., Bathgate, R. A. D., & Summers, R. J. (2006). “Relaxin” the stiffened heart and arteries: The therapeutic potential for relaxin in the treatment of cardiovascular disease. *Pharmacology and Therapeutics*. <http://doi.org/10.1016/j.pharmthera.2005.05.012>

- Senatore, A., Guan, W., & Spafford, J. D. (2014). Cav3 T-type channels: Regulators for gating, membrane expression, and cation selectivity. *Pflügers Archiv European Journal of Physiology*. <http://doi.org/10.1007/s00424-014-1449-7>
- Sharma, U. C., Pokharel, S., Van Brakel, T. J., Van Berlo, J. H., Cleutjens, J. P. M., Schroen, B., ... Pinto, Y. M. (2004). Galectin-3 marks activated macrophages in failure-prone hypertrophied hearts and contributes to cardiac dysfunction. *Circulation*, *110*(19), 3121–3128. <http://doi.org/10.1161/01.CIR.0000147181.65298.4D>
- Shi, Y. (2002). Mechanisms of caspase activation and inhibition during apoptosis. *Molecular Cell*. [http://doi.org/10.1016/S1097-2765\(02\)00482-3](http://doi.org/10.1016/S1097-2765(02)00482-3)
- Stanley, W. C., Recchia, F. a., & Lopaschuk, G. D. (2005). Myocardial substrate metabolism in the normal and failing heart. *Physiological Reviews*, *85*(3), 1093–1129. <http://doi.org/10.1152/physrev.00006.2004>
- Su, B., & Karin, M. (1996). Mitogen-activated protein kinase cascades and regulation of gene expression. *Current Opinion in Immunology*, *8*(3), 402–411. [http://doi.org/10.1016/s0952-7915\(96\)80131-2](http://doi.org/10.1016/s0952-7915(96)80131-2)
- Szalai, G., Krishnamurthy, R., & Hajnóczky, G. (1999). Apoptosis driven by IP3-linked mitochondrial calcium signals. *EMBO Journal*, *18*(22), 6349–6361. <http://doi.org/10.1093/emboj/18.22.6349>
- Tsutsumi, Y. M., Tsutsumi, R., Horikawa, Y. T., Sakai, Y., Hamaguchi, E., Ishikawa, Y., ... Tanaka, K. (2014). Geranylgeranylacetone protects the heart via caveolae and caveolin-3. *Life Sciences*, *101*(1-2), 43–48. <http://doi.org/10.1016/j.lfs.2014.02.019>

- Tuttolomondo, A., Simonetta, I., & Pinto, A. (2016). MicroRNA and receptor mediated signaling pathways as potential therapeutic targets in heart failure. *Expert Opinion on Therapeutic Targets*, 8222(August), 1–14. <http://doi.org/10.1080/14728222.2016.1212017>
- Upadhyay, R., Robay, A., Fakhro, K., Khalil, C. A., Zirie, M., Jayyousi, A., ... Ding, H. (2015). Role of SLMAP genetic variants in susceptibility of diabetes and diabetic retinopathy in Qatari population. *Journal of Translational Medicine*, 13(1), 1–9. <http://doi.org/10.1186/s12967-015-0411-6>
- van den Borne, S. W. M., Diez, J., Blankesteyn, W. M., Verjans, J., Hofstra, L., & Narula, J. (2010). Myocardial remodeling after infarction: the role of myofibroblasts. *Nature Reviews. Cardiology*, 7(1), 30–37. <http://doi.org/10.1038/nrcardio.2009.199>
- Webster, K. A. (2012). Mitochondrial membrane permeabilization and cell death during myocardial infarction: roles of calcium and reactive oxygen species. *Future Cardiol*, 8(6), 863–884. <http://doi.org/10.2217/fca.12.58>
- Wencker, D., Chandra, M., Nguyen, K., Miao, W., Garantziotis, S., Factor, S. M., ... Kitsis, R. N. (2003). A mechanistic role for cardiac myocyte apoptosis in heart failure. *Journal of Clinical Investigation*, 111(10), 1497–1504. <http://doi.org/10.1172/JCI200317664>
- Weng, J. H., Hsieh, Y. C., Huang, C. C. F., Wei, T. Y. W., Lim, L. H., Chen, Y. H., ... Tsai, M. D. (2015). Uncovering the Mechanism of Forkhead-Associated Domain-Mediated TIFA Oligomerization That Plays a Central Role in Immune Responses. *Biochemistry*, 54(40), 6219–6229. <http://doi.org/10.1021/acs.biochem.5b00500>
- Whelan, R. S., Konstantinidis, K., Wei, A.-C., Chen, Y., Reyna, D. E., Jha, S., ... Kitsis, R. N.

(2012). Bax regulates primary necrosis through mitochondrial dynamics. *Proceedings of the National Academy of Sciences of the United States of America*, 109(17), 6566–71.

<http://doi.org/10.1073/pnas.1201608109>

Wielowieyski, P. A., Sevinc, S., Guzzo, R., Salih, M., Wigle, J. T., & Tuana, B. S. (2000).

Alternative splicing, expression, and genomic structure of the 3' region of the gene encoding the sarcolemmal-associated proteins (SLAPs) defines a novel class of coiled-coil tail-anchored membrane proteins. *Journal of Biological Chemistry*, 275(49), 38474–38481.

<http://doi.org/10.1074/jbc.M007682200>

Wigle, J. T., Demchyshyn, L., Pratt, M. A. C., Staines, W. A., Salih, M., & Tuana, B. S. (1997).

Molecular cloning, expression, and chromosomal assignment of sarcolemmal-associated proteins: A family of acidic amphipathic α -helical proteins associated with the membrane. *Journal of Biological Chemistry*, 272(51), 32384–32394.

<http://doi.org/10.1074/jbc.272.51.32384>

Wilde, A. A. M., Antzelevitch, C., Borggrefe, M., Brugada, J., Brugada, R., Brugada, P., ...

Towbin, J. A. (2002). Proposed Diagnostic Criteria for the Brugada Syndrome. *Circulation*, 106(19), 2514–2519. Retrieved from

<http://circ.ahajournals.org/content/106/19/2514.abstract>

Woodman, S. E., Park, D. S., Cohen, A. W., Cheung, M. W. C., Chandra, M., Shirani, J., ...

Lisanti, M. P. (2002). Caveolin-3 knock-out mice develop a progressive cardiomyopathy and show hyperactivation of the p42/44 MAPK cascade. *Journal of Biological Chemistry*, 277(41), 38988–38997. <http://doi.org/10.1074/jbc.M205511200>

Wright, P. T., Nikolaev, V. O., O'Hara, T., Diakonov, I., Bhargava, A., Tokar, S., ... Gorelik, J.

- (2014). Caveolin-3 regulates compartmentation of cardiomyocyte beta2-adrenergic receptor-mediated cAMP signaling. *Journal of Molecular and Cellular Cardiology*, 67, 38–48. <http://doi.org/10.1016/j.yjmcc.2013.12.003>
- Xiao, Q., Hou, N., Wang, Y.-P., He, L.-S., He, Y.-H., Zhang, G.-P., ... Luo, J.-D. (2012). Impaired sonic hedgehog pathway contributes to cardiac dysfunction in type 1 diabetic mice with myocardial infarction. *Cardiovascular Research*, 95(4), 507–16. <http://doi.org/10.1093/cvr/cvs216>
- Yeh, C., Li, H., Malhotra, D., Turcato, S., Nicholas, S., Tu, R., ... Mann, M. J. (2012). NIH Public Access, 109(6), 1185–1191. <http://doi.org/10.1002/jcb.22498>. Distinctive
- Yin, G., Yan, C., & Berk, B. C. (2003). Angiotensin II signaling pathways mediated by tyrosine kinases. *International Journal of Biochemistry and Cell Biology*. [http://doi.org/10.1016/S1357-2725\(02\)00300-X](http://doi.org/10.1016/S1357-2725(02)00300-X)
- Zhang, S., Shi, L., Ma, H., Li, H., Li, Y., Lu, Y., ... Li, W. (2016). Dihydroartemisinin induces apoptosis in human gastric cancer cell line BGC-823 through activation of JNK1/2 and p38 MAPK signaling pathways. *Journal of Receptors and Signal Transduction*, 9893(August), 1–7. <http://doi.org/10.1080/10799893.2016.1203942>
- Zhu, H. (2016). Forkhead box transcription factors in embryonic heart development and congenital heart disease. *Life Sciences*, 144, 194–201. <http://doi.org/10.1016/j.lfs.2015.12.001>
- Rubin, E., Gorstein, F., Rubin, R., Schwarting R., & Strayer, D. (2005). *Rubin's Pathology*.